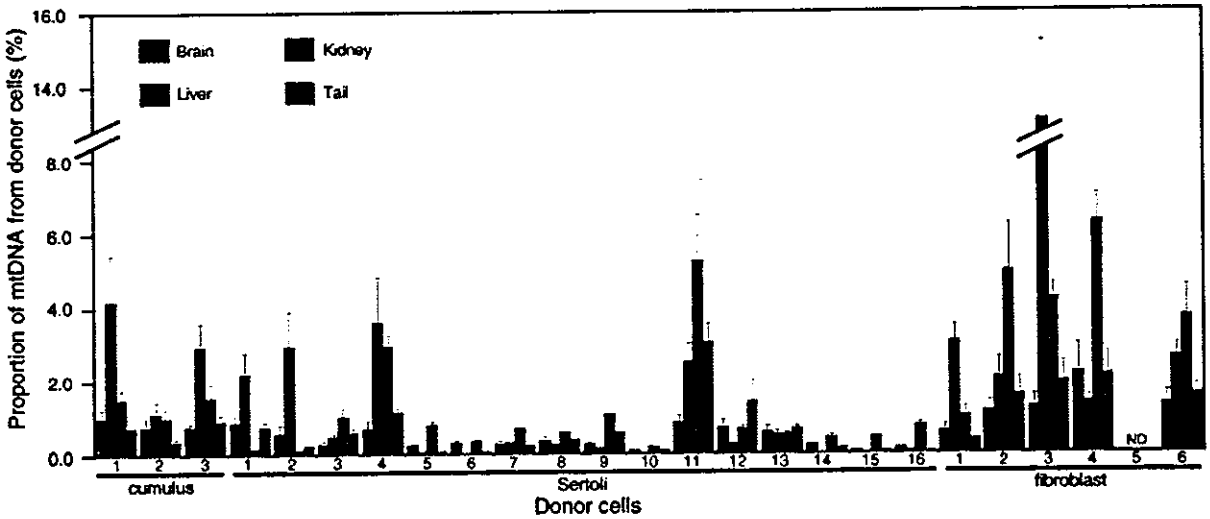

FIG. 2. The levels of mtDNA heteroplasmy in the tissues of mice cloned from different donor cell types. The bars indicate the average proportions of donor cell mtDNAs, and the error bars represent the standard errors. ND, not detected.

external controls were >0.998, and these values were maintained even in the presence of genomic DNA (data not shown). The proportions of donor cell mtDNAs in the tissues from cloned mice are summarized in Figure 2. The values ranged from 0% (all tissues in fibroblast #5) to 13.1% (liver in fibroblast #3). The former corresponds to the clone that lacked donor mtDNA in the nested PCR experiment (lane 3 for fibroblast in Fig. 1b). The latter was also detected by Southern blot analysis (data not shown). Before nuclear transfer, the ratios of single cumulus, Sertoli, and tail tip cells to oocyte mtDNA copy number were approximately 0.5%, 0.5%, and 0.6%, respectively.

ANOVA analysis revealed that mtDNA distribution was dependent on both the donor cell type and the tissue examined. The post-hoc test indicated that there were significantly different outcomes using Sertoli (0.78 ± 0.19% [mean ± SE]) or tail tip fibroblast (2.4 ± 0.7%) cells as donor cells ($P < 0.05$), and between brain (0.6 ± 0.1%) and liver (1.7 ± 0.5%) tissues ($P < 0.05$) (Fig. 2).

We also performed donor cell mtDNA quantification for 20 placentas (two cumulus clones, 14 Sertoli clones, and six fibroblast clones) from the cloned mice. Exact one-to-one correspondence of cloned mice and their placentas was not achieved because some of the cloned offspring were born naturally. All (n = 20) of the examined cloned placentas contained donor mtDNA; this analysis could not be performed for the mouse that lacked the donor mtDNA due to its natural delivery. The average proportions of donor mtDNA were 0.15 ± 0.10% (cumulus cells), 0.24 ± 0.02% (Sertoli cells), and 0.54 ± 0.24% (fibroblasts). Although these values were not significantly different ($P > 0.05$; one-way ANOVA), the use of tail tip fibroblasts generated the highest proportion of donor mtDNA, as was the case for adult animals.

In cloned adults, the proportion of donor mtDNA varies greatly according to the tissue and the individual animal. Two-way ANOVA analysis revealed that there was a significant cell-type effect on donor mtDNA segregation ($P < 0.05$). More of the donor mtDNA copies were transmitted to cloned animals from tail tip cells (fibroblasts) than from cumulus cells or immature Sertoli cells. As mentioned above, there was no difference in the original mtDNA copy numbers in these donor cells. The most likely cause of this donor-cell dependency is the different nuclear transfer methods employed; the cumulus and Sertoli cells were transferred by injection, while the tail tip fibroblasts were transferred by electrofusion. The injection method responded to specific needs of these donor cells, which are too small to be fused by electrofusion. It is assumed that nuclear transfer by injection damages or discards some of the donor mitochondria, while nuclear transfer by electrofusion introduces all donor mitochondria into the recipient oocytes safely. We have previously succeeded in establishing a strain of transmitochondrial mice by electrofusing donor cytoplasts and recipient embryos, but not by direct injection of isolated donor mitochondria into the embryo cytoplasm (Inoue *et al.*, 2000). Nevertheless, the present study demonstrates that nuclear transfer by injection also causes mtDNA heteroplasmy in cloned animals.

Another interesting finding to come out of this study is the presence of statistically significant ($P < 0.05$) tissue-specific selection for donor mtDNA in cloned animals. The post-hoc test demonstrated that there was a significant difference between brain (0.6 ± 0.1%) and liver (1.7 ± 0.5%) tissues in terms of their donor mtDNA content. Although the exact reason for this tissue-specific selection is not known, the possibility of interaction between the nuclear and mitochondrial genomes has

been proposed. Jenuth *et al.* (1997) examined the segregation patterns of tissues in NZB × BALB/c mtDNA-heteroplasmic mice and found a selective increase in the NZB mtDNA genotype in the liver and kidney tissues of mice that had the BALB/c nuclear background. In addition, they demonstrated that the relative proportion of NZB mtDNA increased significantly in an age-dependent manner from the basal level at birth, which indicates that this selective shift occurs postnatally. More recently, Battersby *et al.* (2003) used quantitative trait loci (QTL) analysis to identify three loci that accounted for the selective segregation of certain mtDNA genotypes. They used an intercross with the subspecies *Mus musculus castaneus* to produce F2 progeny, and again found strong mtDNA selection in the liver. Although the mechanism underlying the tissue-specific segregation behaviors of different mtDNA genotypes remains unknown, a similar nuclear genome-driven mechanism recognizing intersubspecies mtDNA differences may operate in our cloned mouse. However, the pattern of the tissue-specific mtDNA distribution may vary with the combination of donor genotype and recipient genotype.

We also analyzed the donor mtDNA content in the cloned placenta, which was the only tissue examined at birth. All of the placentas examined contained donor mtDNA. The range (0.03–1.7%) of the nuclear donor mtDNA contribution in the placenta was consistent with a previous study that showed neutral segregation of mtDNA throughout embryo/fetal development until birth (Jenuth *et al.*, 1997). It would be interesting to see whether age-related selection of mtDNA genotypes applies equally to nuclear-transferred mice and experimentally produced heteroplasmic mice.

In conclusion, we first demonstrated the steady-state inheritance of donor mtDNA into cloned mice. The quantitative mtDNA analysis was sufficiently consistent to obtain statistically significant results by ANOVA analysis with a complete factorial design (three donor cell types × four tissues examined). These clear-cut results may be attributable to the biological homogeneity of genetically defined laboratory mice. Thus, this experimental system provides valuable information on extranuclear genetic influences on the biological characteristics of cloned animals.

MATERIALS AND METHODS

Nuclear Transfer

Nuclear transfer was carried out as described previously (Wakayama *et al.*, 1998; Ogura *et al.*, 2000a, b). The oocytes were collected from 8-week-old B6D2F1 females that were superovulated by injection with PMSG (7.5 IU) and hCG (7.5 IU) at 48-h intervals. At 15 h after the hCG injection, cumulus-oocyte complexes were collected from the oviducts and the cumulus cells were allowed to disperse in KSOM medium (Lawitts and Biggers, 1993) that contained 0.1% bovine testicular hyaluronidase. The oocytes were enucleated in Hepes-buffered KSOM medium that contained 7.5 μg/ml cytochalasin B (Calbiochem, San Diego, CA). The nuclei from the cumulus and Sertoli cells were transferred into enucleated oocytes together with the cytoplasm using intracytoplasmic injection with piezo-driven micromanipulators (Prime Tech, Ibaraki, Japan) in Hepes-buffered KSOM. Tail tip fibroblasts were transferred by electrofusion using the LF101 electric pulse generator (Nepa Gene, Chiba, Japan). After nuclear transfer, the oocytes were activated and cultured in KSOM, as described previously (Inoue *et al.*, 2003). Embryos that developed to morulae or blastocysts after 72 h in culture were transferred into the uteri of day-2.5 pseudopregnant ICR females. The cloned pups were retrieved from day-19.5 recipient females by cesarean section or through natural delivery.

Qualitative and Quantitative Analyses of MtDNA in Cloned Animals

Tissue samples for mtDNA analysis were collected from the brain, liver, kidney, and tail of adult animals (115–403 days of age), and from the placenta of newborn animals. The allele-specific primer sets used for the amplification of mtDNA of either origin are shown in Figure 1. The forward primers were: D1, 5′-AGTACATTAAATCAATGGTTC-3′; D2, 5′-AATAATCATCAACATAAATCA-3′; M1, 5′-AGTACATTTAATCAATGATAT-3′; and M2, 5′-AACAATTATCAACATAAACTG-3′. The reverse primers were: C1, 5′-TGGGCCCGGAGCGAGAAGAGG-3′; and C2, 5′-TCACGGAGGATGGTAGA-3′. The D1 and D2 primers were used for amplification of the *M. m. domesticus* mtDNA, the M1 and M2 primers were used for the *M. m. molossinus* mtDNA, and the C1 and C2 primers were used for both mtDNA species. Nested PCR to detect low amounts of mtDNA from donor cells was carried out with M1 and C1 as the first primer pair and M2 and C2 as the second primer pair. PCR was performed with an initial activation step of 94°C for 5 min, followed by 30 cycles of denaturation at 94°C for 1 min, annealing at 50°C for 1 min, and extension at 72°C for 1 min.

The PCR products that were amplified with primer sets D1 and C1 or M1 and C1 were cloned into the pPCR-Script Amp SK(+) vector using the PCR-Script Amp Cloning Kit (Stratagene, La Jolla, CA). The recombinant plasmids were purified and their concentrations were determined by measuring the absorption at 260 nm in a spectrophotometer. Serial dilutions of the DNA were then made to assess the concentration of a known number of templates. These serial dilutions were used as the external standards for the real-time PCR.

The ABI Prism 7900HT was used to determine the levels of mtDNA of different origins using the Quanti-Tect Syber Green PCR Kit (Qiagen, Hilden, Germany). After an initial activation step at 50°C for 2 min and denaturation at 95°C for 15 min, PCR was carried out for 35 cycles of 95°C for 15 s, 50°C for 30 s, and 72°C for 30 s. All of the samples were assayed three times. For each run a standard curve was generated using six 10-fold serial dilutions of the external standard. The threshold cycle (Ct) allowed determination of the starting

amount of template mtDNA in each sample. We calculated the amount of JF1 mtDNA relative to the total mtDNA level.

Statistical Analysis

The proportions of JF1 mtDNA genotypes were transformed by arcsine transformation and analyzed by repeated-measure ANOVA using a 3 (donor cell type) × 4 (tissue) factorial design. The Bonferroni/Dunn post-hoc test was performed for multiple comparisons of the groups, as appropriate. Unlike the samples that were collected from adult clones, the placentas were collected at birth, and therefore they were subjected to a separate statistical analysis from the other adult tissues.

LITERATURE CITED

Baarends WM, Hoogerbrugge JW, Roest HP, Ooms M, Vreeburg J, Hoeijmakers JH, Grootegoed JA. 1999. Histone ubiquitination and chromatin remodeling in mouse spermatogenesis. Dev Biol 207: 322-333.

Battersby BJ, Loredo-Osti JC, Shoubridge EA. 2003. Nuclear genetic control of mitochondrial DNA segregation. Nat Genet 33:183-186.

Chen HY, Sun JM, Zhang Y, Davie JR, Meistrich ML. 1998. Ubiquitination of histone H3 in elongating spermatids of rat testes. J Biol Chem 273:13165-13169.

Evans MJ, Gurer C, Loike JD, Wilmut I, Schnieke AE, Schon EA. 1999. Mitochondrial DNA genotypes in nuclear transfer-derived cloned sheep. Nat Genet 23:90-93.

Galli C, Lagutina I, Crotti G, Colleoni S, Turini P, Ponderato N, Duchi R, Lazzari G. 2003. A cloned horse born to its dam twin. Nature 424:635.

Hiendleder S, Zakhartchenko V, Wenigerkind H, Reichenbach HD, Bruggerhoff K, Prelle K, Brem G, Stojkovic M, Wolf E. 2003. Heteroplasmy in bovine fetuses produced by intra- and interspecific somatic cell nuclear transfer: neutral segregation of nuclear donor mitochondrial DNA in various tissues and evidence for recipient cow mitochondria in fetal blood. Biol Reprod 68: 159-166.

Inoue K, Nakada K, Ogura A, Isobe K, Goto Y, Nonaka I, Hayashi JI. 2000. Generation of mice with mitochondrial dysfunction by introducing mouse mtDNA carrying a deletion into zygotes. Nat Genet 26:176-181.

Inoue K, Kohda T, Lee J, Ogonuki N, Mochida K, Noguchi Y, Tanemura K, Kaneko-Ishino T, Ishino F, Ogura A. 2002. Faithful expression of imprinted genes in cloned mice. Science 295:297.

Inoue K, Ogonuki N, Mochida K, Yamamoto Y, Takano K, Kohda T, Ishino F, Ogura A. 2003. Effects of donor cell type and genotype on the efficiency of mouse somatic cell cloning. Biol Reprod 69:1394-1400.

Jenuth JP, Peterson AC, Shoubridge EA. 1997. Tissue-specific selection for different mtDNA genotypes in heteroplasmic mice. Nat Genet 16:93-95.

Kaneda H, Hayashi J, Takahama S, Taya C, Lindahl KF, Yonekawa H. 1995. Elimination of paternal mitochondrial DNA in intraspecific crosses during early mouse embryogenesis. Proc Natl Acad Sci USA 92:4542-4546.

Lawitts JA, Biggers JD. 1993. Culture of preimplantation embryos. Methods Enzymol 225:153-164.

Meirelles FV, Bordignon V, Watanabe Y, Watanabe M, Dayan A, Lobo RB, Garcia JM, Smith LC. 2001. Complete replacement of the mitochondrial genotype in a *Bos indicus* calf reconstructed by nuclear transfer to a *Bos taurus* oocyte. Genetics 158:351-356.

Ogura A, Inoue K, Ogonuki N, Noguchi A, Takano K, Nagano R, Suzuki O, Lee J, Ishino F, Matsuda J. 2000a. Production of male cloned mice from fresh, cultured, and cryopreserved immature Sertoli cells. Biol Reprod 62:1579-1584.

Ogura A, Inoue K, Takano K, Wakayama T, Yanagimachi R. 2000b. Birth of mice after nuclear transfer by electrofusion using tail tip cells. Mol Reprod Dev 57:55-59.

Ogura A, Ogonuki N, Takano K, Inoue K. 2001. Microinsemination, nuclear transfer, and cytoplasmic transfer: the application of new reproductive engineering techniques to mouse genetics. Mamm Genome 12:803-812.

Ogura A, Inoue K, Ogonuki N, Lee J, Kohda T, Ishino F. 2002. Phenotypic effects of somatic cell cloning in the mouse. Cloning Stem Cells 4:397-405.

Steinborn R, Schinogl P, Zakhartchenko V, Achmann R, Schernthaner W, Stojkovic M, Wolf E, Muller M, Brem G. 2000. Mitochondrial DNA heteroplasmy in cloned cattle produced by fetal and adult cell cloning. Nat Genet 25:255-257.

Steinborn R, Schinogl P, Wells DN, Bergthaler A, Muller M, Brem G. 2002. Coexistence of *Bos taurus* and *B. indicus* mitochondrial DNAs in nuclear transfer-derived somatic cattle clones. Genetics 162:823-829.

Sutovsky P, Moreno RD, Ramalho-Santos J, Dominko T, Simerly C, Schatten G. 1999. Ubiquitin tag for sperm mitochondria. Nature 402:371-372.

Sutovsky P, Moreno RD, Ramalho-Santos J, Dominko T, Simerly C, Schatten G. 2000. Ubiquitinated sperm mitochondria, selective proteolysis, and the regulation of mitochondrial inheritance in mammalian embryos. Biol Reprod 63:582-590.

Takeda K, Akagi S, Kaneyama K, Kojima T, Takahashi S, Imai H, Yamanaka M, Onishi A, Hanada H. 2003. Proliferation of donor mitochondrial DNA in nuclear transfer calves (*Bos taurus*) derived from cumulus cells. Mol Reprod Dev 64:429-437.

Wakayama T, Perry AC, Zuccotti M, Johnson KR, Yanagimachi R. 1998. Full-term development of mice from enucleated oocytes injected with cumulus cell nuclei. Nature 394:369-374.

Wilmut I, Beaujean N, de Sousa PA, Dinnyes A, King TJ, Paterson LA, Wells DN, Young LE. 2002. Somatic cell nuclear transfer. Nature 419:583-586.

Woods GL, White KL, Vanderwall DK, Li GP, Aston KI, Bunch TD, Meerdo LN, Pate BJ. 2003. A mule cloned from fetal cells by nuclear transfer. Science 301:1063.

BIOLOGY OF REPRODUCTION 70, 1213–1221 (2004)
Published online before print 26 December 2003.
DOI 10.1095/biolreprod.103.024802

The Novel Dominant Mutation *Dspd* Leads to a Severe Spermiogenesis Defect in Mice[1]

Masayuki Kai,[4,5] Masahito Irie,[4] Tomohisa Okutsu,[3,4] Kimiko Inoue,[5,6] Narumi Ogonuki,[5,6] Hiromi Miki,[6] Minesuke Yokoyama,[5,7] Rika Migishima,[7] Kaori Muguruma,[8] Hisako Fujimura,[9] Takashi Kohda,[4,5] Atsuo Ogura,[5,6] Tomoko Kaneko-Ishino,[5,10] and Fumitoshi Ishino[2,5,11]

Division for Gene Research,[4] Center for Biological Resources and Informatics, Tokyo Institute of Technology, Midori-ku, Yokohama 226-8501, Japan
CREST,[5] Japan Science and Technology Agency (JST), Kawaguchi, Saitama 332-0011, Japan
BioResource Center,[6] RIKEN, Tsukuba, Ibaraki 305-0074, Japan
Mitsubishi Kagaku Institute of Life Sciences,[7], Tokyo 194-8511, Japan
Central Institute for Experimental Animals,[8] Miyamae-ku, Kawasaki 216-0001, Japan
Exploratory Toxicology and DMPK Research Laboratories,[9] Tanabe Seiyaku Co., Ltd., Chuo-ku, Osaka 541-8505, Japan
School of Health Sciences,[10] Tokai University, Bohseidai, Isehara, Kanagawa 259-11, Japan
Medical Research Institute,[11] Tokyo Medical and Dental University, Chiyoda-ku, Tokyo 101-0062, Japan

ABSTRACT

Spermiogenesis is a complex process that is regulated by a plethora of genes and interactions between germ and somatic cells. Here we report a novel mutant mouse strain that carries a transgene insertional/translocational mutation and exhibits dominant male sterility. We named the mutation dominant spermiogenesis defect (*Dspd*). In the testes of *Dspd* mutant mice, spermatids detached from the seminiferous epithelium at different steps of the differentiation process before the completion of spermiogenesis. Microinsemination using spermatids collected from the mutant testes resulted in the birth of normal offspring. These observations indicate that the major cause of *Dspd* infertility is (are) a defect(s) in the Sertoli cell-spermatid interaction or communication in the seminiferous tubules. Fluorescent in situ hybridization (FISH) analysis revealed a translocation between chromosomes 7F and 14C at the transgene insertion site. The deletion of a genomic region of chromosome 7F greater than 1 megabase and containing at least six genes (*Cttn, Fadd, Fgf3, Fgf4, Fgf15,* and *Ccnd1*) was associated with the translocation. *Cttn* encodes the actin-binding protein cortactin. Immunohistochemical analysis revealed localization of cortactin beside elongated spermatids in wild-type testes; abnormality of cortactin localization was found in mutant testes. These data suggest an important role of cortactin in Sertoli cell-spermatid interactions and in the *Dspd* phenotype.

sertoli cells, spermatid, spermatogenesis

INTRODUCTION

Human infertility is observed in 10–15% of couples and the contributing factors are attributed to males and females equally. Spermatogenic arrest is the major cause of male infertility [1, 2]. The most common cause of spermatogenic arrest identified genetically is a microdeletion of the Y chromosome; however, this deletion accounts for less than 5% of male infertility [3]. There are likely many other autosomal genes and loci that affect spermatogenesis, but only a limited number have been identified.

The random integration of foreign DNA during the production of transgenic mice often leads to genomic rearrangements. Nakanishi et al. reported that chromosomal translocation was observed in about 5% of their EGFP transgenic lines [4]. Translocation is often accompanied by a genomic deletion that can vary enormously in size. It has not been easy to determine the size of deletions, but recently improved mouse genome databases that contain information on single nucleotide polymorphisms (SNPs) provide platforms for the quick size determination of even massive deletions.

A number of mutant mice showing abnormalities in spermatogenesis, including some insertional mutants [5–7], have provided important models for male infertility [3]. However, much remains to be understood. One of the obstacles to the analysis of spermatogenesis is that the spermatogenic process has not been reproduced in vitro [8]. The interaction between somatic Sertoli cells and germ cells is an important factor in spermatogenesis, making it difficult to reconstitute spermatogenesis in vitro. Sertoli cells are multifunctional nurse cells that provide nutritional and physical support for spermatogenic cells throughout sperm development. The Sertoli cell-spermatid interaction in particular is thought essential for the formation of a normal sperm head and for the release of sperm at the correct time. Filamentous (F-) actin plays an important role in Sertoli cell-spermatid interactions. The ectoplasmic specialization (ES) [9], a specialized junctional structure between Sertoli cells and elongated spermatids after step 8, contains an actin layer [10, 11]. The ES is damaged by treatment with the actin-disrupting drug cytochalasin D [12]. Mice treated with bisphenol-A or β-estradiol 3-benzoate exhibit an ab-

[1]This work was supported by grants to F.I. from CREST, the research program of the Japan Science and Technology Agency (JST), the Uehara Memorial Life Science Foundation, and the Ministry of Health, Labour for Child Health and Development (14-C).
[2]Correspondence: Fumitoshi Ishino, Medical Research Institute, Tokyo Medical and Dental University, 2-3-10 Kandasurugadai, Chiyoda-ku, Tokyo 101-0062, Japan. FAX: +81 3 5280 8073; e-mail: fishino.epgn@mri.tmd.ac.jp
[3]Current address: Ajinomoto Co., Inc., 1-1 Suzuki-cho, Kawasaki-ku, Kawasaki, Kanagawa 210-8681, Japan.

Received: 30 October 2003.
First decision: 26 November 2003.
Accepted: 10 December 2003.

ISSN: 0006-3363. http://www.biolreprod.org

normality of the ES. They also show abnormal spermatid morphology and the detachment of spermatids from the seminiferous epithelium, suggesting that an abnormal ES leads to spermatid abnormalities [13].

In this report, we identified a novel insertional/translocational mutation, which we named dominant spermiogenesis defect (*Dspd*), that results in a severe spermiogenesis defect manifested as head dysmorphology in elongated spermatids and a significant decrease in the number of elongated spermatids. Immature spermatids found in the mutant epididymides were released from the seminiferous epithelium inappropriately, suggesting inefficient Sertoli cell-spermatid interactions. The mutation loci of *Dspd* were mapped to two chromosomes (chromosomes 7F [chr.7F] and 14C [chr.14C]) by analyzing the translocation, which produced a genomic deletion of greater than 1 megabase (Mb) in chr.7F. Based on its location within the deleted region of chr.7F and the putative function of its gene product, *Cttn* (cortactin) is the most likely candidate gene responsible for the *Dspd* phenotype. Analysis of *Dspd* may provide a novel approach to understanding the molecular mechanisms and roles of Sertoli cell-spermatid interactions in spermiogenesis.

MATERIALS AND METHODS

All procedures described within were reviewed and approved by Tokyo Institute of Technology Institutional Animal Care and Use Committee and were performed in accordance with the Guiding Principles for the Care and Use of Laboratory Animals.

Transgenic Mice

The full-length human *PEG8* cDNA (GenBank Accession Number AB030733) [14] was cloned downstream from the cytomegalovirus immediate early (CMV-IE) enhancer and the chicken β-actin promoter (Fig. 1A). The DNA was injected into the male pronuclei of (C57BL/6 × C3H) F_1 eggs using standard techniques. The transgenic mice were selected after screening the tail DNA by Southern-blot analysis using ^{32}P-labeled human *PEG8* cDNA as a probe.

Mating of Mice

The founder female (1L) was mated to a male C57BL/6 mouse, and two male offspring having the transgene were obtained. The two F_1 males, at 3–6 mo of age, were mated to C57BL/6 females. They made 11 vaginal plugs; however, no offspring were obtained after natural matings.

Microinsemination

Spermatogenic cells were collected from recipient *Dspd*/wt male mice and frozen, as described previously [15, 16]. After thawing, elongated and round spermatids were directly injected into the ooplasm of wild-type mature oocytes using a Piezo-driven micromanipulator. Mature oocytes were collected from B6D2F1 females, which had been superovulated by injection with 5 IU of eCG followed 48 h later by 5 IU of hCG. Fertilized oocytes were cultured for 48 h, and four- to eight-cell embryos were transferred into the oviducts of pseudopregnant ICR females on the day following sterile mating with vasectomized ICR males.

Reverse Transcription-Polymerase Chain Reaction

Total RNA was prepared from the testes of *Dspd*/wt mice and another *PEG8* transgenic mouse using ISOGEN (Nippon Gene, Toyama, Japan); cDNA was synthesized from 1 μg of total RNA using SuperscriptII reverse transcriptase (Life Technologies, Grand Island, NY) and an oligo(dT) primer. The polymerase chain reaction (PCR) was performed with *EX Taq* DNA polymerase (Takara, Kyoto, Japan). The primers for *PEG8* amplification were *PEG8*-F: 5′-TGGACACACAGCTCTGCTTG-3′ and *PEG8*-R: 5′-CCTGGGAATGCTCATTCATG-3′.

Western Blot Analysis

Recombinant His-tagged PEG8 (His-PEG8) protein was produced in *Escherichia coli* and purified with Probond Nickel-Chelating Resin (Invitrogen, San Diego, CA). Rabbits were immunized with the purified His-PEG8 protein. The polyclonal antiserum was collected and used for Western blot analyses. Whole cell extract (WCE) was prepared from adult testes. WCE samples containing 10 μg of total proteins were electrophoresed on 10% SDS-polyacrylamide gels and electroblotted to Hybond-P membranes (Amersham, Tokyo, Japan). His-PEG8 was used as a positive control. The enhanced chemiluminescence Western blotting detection system (Amersham) was used to visualize the results.

Histological Examination

For light microscopic examination, testes and epididymides were fixed in Bouin solution (Sigma, St. Louis, MO) and embedded in paraffin using standard techniques. Sections (3–4 μm) were cut, deparaffinized in xylene, rehydrated with a series of ethanol solutions, and stained with hematoxylin-eosin. Fifteen *Dspd*/wt mice were examined by light microscopy, and they showed the same phenotype. The numbers of spermatids per tubule at stages I–VI (steps 13–15) and at stages VII–VIII (step 16) were counted under light microscopy. Ten tubules of each stage (stages I–VI and stages VII–VIII) per testis were examined. Three mice for each genotype (*Dspd*/wt and wt/wt) were examined. Statistical analysis was performed by the unpaired *t*-test.

For electron microscopic examination, small blocks of testes were immersed in 2.5% glutaraldehyde, 2% paraformaldehyde in 0.1 M phosphate buffer (pH 7.3), and postfixed with 1% osmium tetraoxide. After dehydration, specimens were embedded in Epon/Araldite. Ultrathin sections were prepared, stained with uranyl acetate and lead citrate, and examined with an electron microscope (JEM-1210; JEOL, Tokyo, Japan). Four *Dspd*/wt mice were examined by electron microscopy, and they showed the same phenotype.

Fluorescent In Situ Hybridization (FISH)

Fluorescent in situ hybridization (FISH) was performed using a standard method, using the entire transgene as a probe. One F_1 male and one F_3 female (marked with asterisks [*] in Fig. 1B) having the transgene were examined. They had the same karyotypes, except for the sex chromosomes.

Genomic Library Screening

Genomic DNA was prepared from a *Dspd*/wt mouse, partially digested with the restriction enzyme *Sau*3AI, and ligated into the cosmid vector Supercos 1 (Stratagene, La Jolla, CA), which had been digested previously with *Xba*I and *Bam*HI. After it was packaged (Gigapack III XL; Stratagene), the phage was used to transfect *E. coli* XL1-blue. The cosmid library was screened using *PEG8* cDNA as a probe.

Genomic Deletion Analysis Using Single Nucleotide Polymorphisms

(DBA2 × C57BL/6) F_1 mutant mice were produced by the microinsemination of eggs from superovulated DBA2 females with spermatogenic cells from a male *Dspd*/wt (C57BL/6 background) mouse. Genomic DNA from three transgene-positive F_1 mice and three transgene-negative F_1 mice (wild-type controls) was prepared. DNA fragments containing polymorphisms between DBA2 and C57BL/6 were amplified by PCR using the primers listed below, which are based on sequences in the Mouse RefSNP database (Celera Discovery System, Celera Genomics, http://www.celera.com). The PCR products were analyzed by direct sequencing. All three transgene-positive F_1 mice gave the same results.

Primer sets for chromosome 7. mCV24660825: 5′-CATGGGACTGTGATGGTAAC-3′ and 5′-GCATGTGTATCTGCTCAAGG-3; mCV24854750: 5′-ACACGCAGATGCTCTGTAG-3′ and 5′-ATGTATCTAACAGTGAAGGCC-3′; mCV23705239: 5′-GAAGCATGCAAACACAGC-3′ and 5′-GTAAAGTCTGTGGTGCAGTG-3′; mCV22810840: 5′-GCTGCTTTGACTTCTGCTC-3′ and 5′-AACTCTCCCAGGTTTGTT-3′; mCV24856115: 5′-CCATGTATCAAAGCCAGG-3′ and 5′-GATCTGTCATTGAGTGTACCC-3′; mCV24317904: 5′-TCGGAGCAGTAACTCTGTG-3′ and 5′-GGAGTACAGGTACTGCAGG-3′; mCV22532403: 5′-GCAGGAGGTCACACTAAGC-3′ and 5′-AGTAAATGCAGAAATAGCTGG-3′; and mCV22989836: 5′-CCAAGGTTTCCAACAAAAG-3′ and 5′-ACCACCACCTATGTGATCAG-3′.

Primer sets for chromosome 14. mCV24975960: 5′-CAACTGTGTCACAGTATGG-3′ and 5′-GGTTTCTGGTGATTGTGG-3′; mCV22764767: 5′-CTCCTGCTGTGATTGATCTC-3′ and 5′-TGCAGAGGATGAAAGATTGG-3′; mCV24986264: 5′-TGTGCACACTGTAACAAACC-3′

and 5′-GCACTGTTTTGCATTGTTCC-3′; mCV24616564: 5′-CTGCAG CCATAAAACTTCC-3′ and 5′-CAAGGGTCTTTATCACCAC-3′; and mCV23859822: 5′-TTCAGGTTGCTTGTAAGCC-3′ and 5′-TAAGCAG GAGTGATTGCTG-3′.

Immunohistochemistry

Testes removed from adult mice were fixed overnight in 20% (v/v) formalin containing 5% sucrose. They were embedded in paraffin using standard techniques and sections (3–4 μm) were prepared. Sections were deparaffinized in xylene, rehydrated through a series of ethanol solutions, boiled in 1 mM EDTA to activate antigens, treated with 1% H_2O_2 to block endoperoxidases, and incubated in 5% (v/v) normal goat serum in PBS. Sections were reacted with anti-cortactin rabbit polyclonal antibody (#3502; Cell Signaling Technology, Beverly, MA) at dilution 1:50, visualized with anti-rabbit Envision Plus (DAKO, Glostrup, Denmark), and counterstained with methylgreen.

RESULTS

Four lines of transgenic mice (1L, 11L, 16L, and 19L) carrying the human *PEG8* transgene [14] (Fig. 1A) were produced. Male infertility was observed only in 1L progenies; two F_1 males inherited the transgene (Tg) from a founder female mouse and were infertile (Fig. 1B). No phenotypic abnormalities were observed in the other transgenic lines expressing the *PEG8* message (Fig. 1C; 11L and 19L), and no detectable PEG8 protein was produced in the testes of 1L or 19L mice (Fig. 1D). Therefore, we concluded that the infertility observed in the 1L line was not caused by PEG8 expression, but by an insertional mutation of the transgene. The two affected F_1 males had few mature spermatozoa in the cauda epididymidis, and no offspring were obtained after natural mating although 11 vaginal plugs (total number from the two F_1 males) were recorded. We could not perform in vitro fertilization due to the inability of retrieving spermatozoa from the epididymidis of F_1 heterozygous males. However, when round and elongated spermatids collected from the mutant testes were injected into oocytes directly (see *Microinsemination* in *Materials and Methods*), normal offspring were obtained (Fig. 1B), indicating that the spermatids had normal haploid genomes. Intracytoplasmic sperm injection enabled us to maintain this mutant strain and to carry out histological and genetic analyses. All the heterozygous males examined were infertile, but wild-type littermates and heterozygous females were fertile and phenotypically normal. However, the litter sizes of heterozygous females in mating with wild-type males were relatively low (average = 3.0, SD = 1.0, n = 12), whereas the ratios Tg(+):(−) and male:female followed the Mendelian law (Tg[+]:[−] = 20:16, male:female = 20:16, 36 offspring). In this study, we have not tried to make homozygous mice because of the infertility of heterozygous males; therefore, phenotype of homozygotes have been unknown; however, they were speculated to be embryonic lethal (see *Discussion*).

Histological analyses were performed to precisely determine the phenotype. Examinations of the testes from heterozygous mutant mice revealed a severe spermiogenesis defect (Fig. 2, A and C). In the mutant testes, round spermatids seemed to be normal, but the number of elongated spermatids was significantly decreased (steps 13–15, $P = 4.3 \times 10^{-10}$; step 16, $P = 6.5 \times 10^{-15}$). In *Dspd*/wt mice, the average number of steps 13–15 spermatids remaining in the epithelium per tubule (stages I–VI) was about 30% of the wild type, and the arrangement of elongated spermatids was disrupted. Some of the elongated spermatids had misshapen heads (inset of Fig. 2C). There were only a few mature (step 16) spermatids at the luminal edge of the

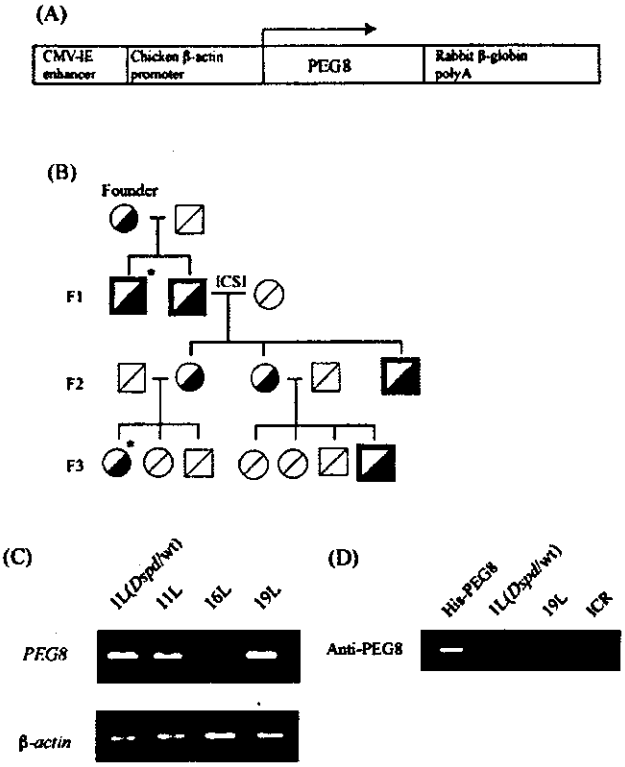

FIG. 1. The *PEG8* transgene and mutant pedigree. **A**) The *PEG8* transgene is composed of the CMV-IE enhancer, chicken β-actin promoter, human *PEG8* cDNA, and rabbit β-globin polyA signal. The length of the construct is 4.5 kilobases. **B**) Pedigree for the 1L line. The squares represent male mice, and circles represent female mice. The half-colored symbols represent mice that inherited the transgene. Asterisks indicate individuals analyzed by FISH. **C**) Transgene expression analysis by RT-PCR using testes of 1L line (heterozygous for the *Dspd* mutation; *Dspd*/wt) and other *PEG8* transgenic lines (11L, 16L, and 19L). In 16L, the level of *PEG8* expression was relatively low. The expression in 1L (*Dspd*/wt) and 19L was similar. **D**) Western blot analysis of testis whole-cell extract with anti-PEG8 antibody. No detectable PEG8 protein was produced in 1L (*Dspd*/wt) or 19L. Recombinant His-tagged PEG8 protein (His-PEG8) was used as a positive control.

seminiferous epithelium. The average number of step 16 spermatids per tubule (stages VII–VIII) was 7.7% of the wild type. In addition, multinucleated spermatids were often found (data not shown). Leydig cells were morphologically normal. In the cauda epididymidis of wild-type males, the lumen was filled with mature spermatozoa (Fig. 2, F and H). By contrast, the number of spermatozoa found in the mutant epididymides was reduced, and almost all spermatozoa had variously misshapen heads (Fig. 2, E and G, arrows). Furthermore, immature spermatids and their debris were seen detached inappropriately from the seminiferous epithelium in the mutant epididymides (Figs. 2G and 3). The detachment of immature spermatids from the seminiferous epithelium is clearly observed in the electron micrographs (Fig. 3). Immature spermatids were found detached from the seminiferous epithelium in the lumens of *Dspd*/wt seminiferous tubules. Elongated spermatids in the lumen had abnormal head shapes, and some of them were often enclosed by a nucleus-free, membrane-bound cytoplasm that was probably Sertoli-cell in origin. Round spermatids were also found in the lumen. The decrease in the number of spermatids suggests that many spermatids are

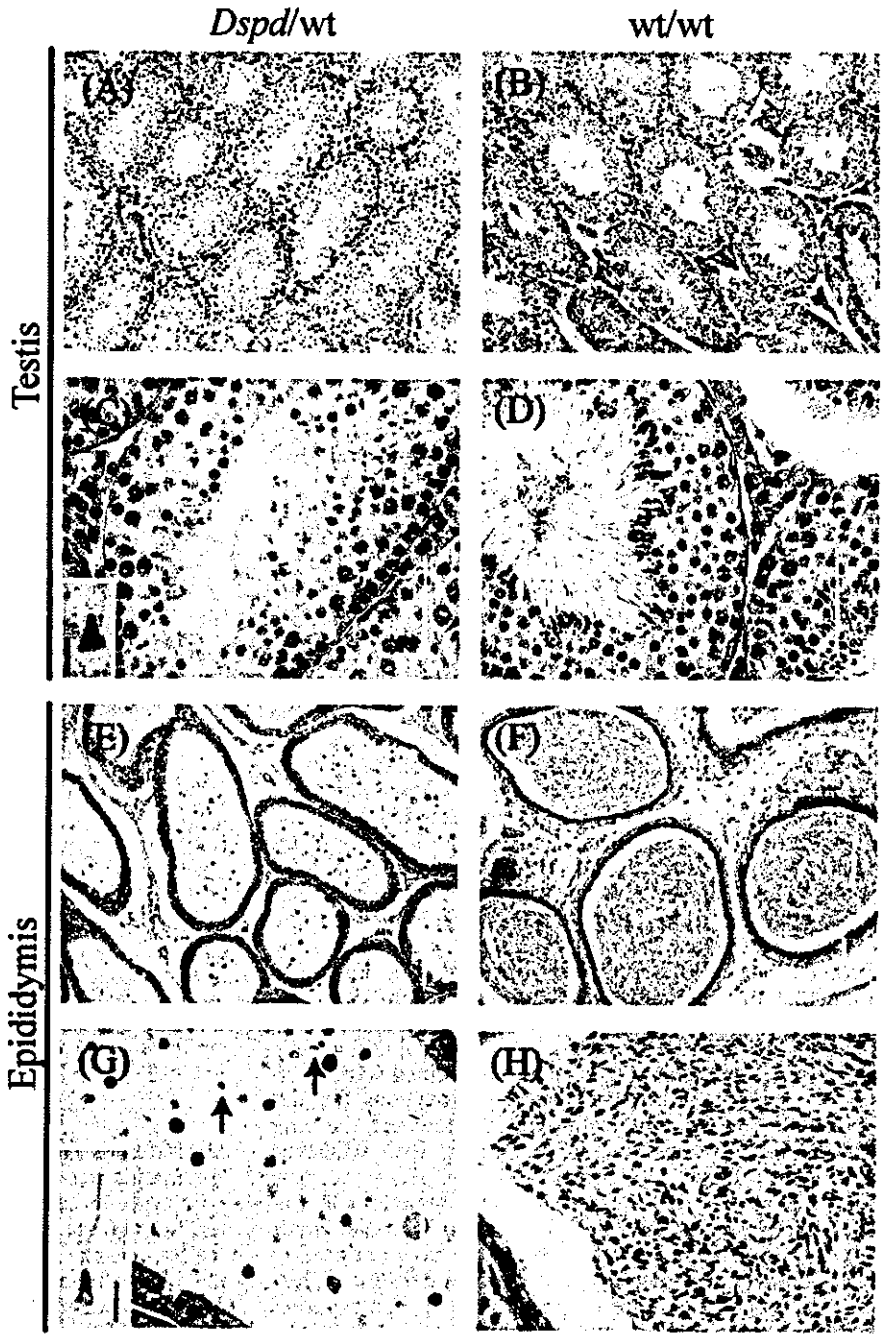

FIG. 2. Light microscopy of the histology of adult testes and epididymides. Seminiferous tubules from a heterozygous *Dspd* mouse (*Dspd*/wt) (**A**, bar = 200 μm; **C**, bar = 100 μm; inset of **C**, bar = 5 μm) and a wild-type littermate (wt/wt) (**B**, bar = 200 μm; **D**, bar = 100 μm) are shown. In *Dspd*/wt seminiferous tubules, Sertoli cells and germ cells from spermatogonia to round spermatids appeared normal; however, there were only a few mature spermatids. Furthermore, misshapen elongated spermatids were frequently found in mutant seminiferous tubules (inset of **C**). The cauda epididymidis from *Dspd*/wt (**E**, bar = 200 μm; **G**, bar = 100 μm) and wt/wt (**F**, bar = 200 μm; **H**, bar = 100 μm) are shown. The wt/wt epididymal tubule was filled with spermatozoa. Much fewer spermatozoa were observed in the mutant epididymal tubule; almost all the spermatozoa had morphologically abnormal sperm heads (**G**, arrows and inset, bar = 5 μm).

detached from the seminiferous epithelium during maturation. Spermatids detached from the seminiferous epithelium at different steps of the differentiation process before the completion of spermiogenesis. There seemed to be no particular step at which detachment of spermatids occurs. Based on these observations, the abnormalities associated with this mutation can be summarized as 1) head dysmorphology of elongated spermatids and 2) detachment of immature spermatids from seminiferous epithelium. Therefore, we named the mutation dominant spermiogenesis defect (*Dspd*) for its genetic and phenotypic features.

The chromosomal localization of the transgene insertion site was determined by FISH using the transgene as a probe. In the mutant mice, a translocation was observed between chr.7F and chr.14C that resulted in a fusion chromosome longer than chr.1 and a short chromosome containing a proximal fragment of chr.14. A signal from the transgene was detected at the junction of the long fused chromosome (Fig. 4A). The same results were obtained with two 1L mice (one F_1 male and one F_3 female, marked by asterisks [*] in Fig. 1B). The low litter size of the mutant females (Fig. 1B) suggests that only offspring inheriting the two mutant chromosomes as a pair can survive.

Next, a genomic library of a *Dspd*/wt mouse was screened using *PEG8* cDNA as a probe. Two clones containing transgene (Tg)-genome junctions were obtained;

FIG. 3. Electron micrograph of *Dspd*/wt seminiferous tubule. Lu, lumen; Epi, epithelium of the seminiferous tubule. Immature spermatids are shown detaching from the seminiferous epithelium. Some elongated spermatids (Sd) were accompanied by cytoplasm that was probably Sertoli-cell in origin, and they had abnormal head morphology. Wandering round spermatids (Rsd) were often found in the lumen. Bar = 5 μm.

Southern-blot analysis confirmed that they were adjacent to the transgene (data not shown). The DNA sequences of the two junction sites were mapped on chr.7 and chr.14 using mouse genome sequence databases (Fig. 4B, red arrows) in conjunction with the FISH results.

To determine whether there were any deletions of the genome at the mutation loci, we carried out SNP analysis between two laboratory mouse strains, C57BL/6 (B6) and DBA2 (D2). Mapping information for the mouse SNPs was provided by Celera Mouse RefSNP database. The (D2 × B6) F_1 mice with the *Dspd* mutation were produced by injecting spermatids of the *Dspd*/wt mice with a B6 background into D2 oocytes. DNA fragments containing SNPs were amplified by PCR and checked by direct sequencing of the PCR products. The results are shown in Figure 4B. We detected both D2 and B6 alleles at all markers analyzed on chr.14. The physical distance from the Tg-genome junction to the nearest marker, mCV24616564, is about 1 Mb. Therefore, these data showed that no deletion greater than 1 Mb occurred at the junction of chr.14. We confirmed that the nearest gene, *Sftpd,* was intact on both alleles. However, the 1-Mb region between mCV24616564 and the Tg-genome junction could not be analyzed because the region consists of highly repetitive sequences and the genomic assembly has not yet been completed. It is unlikely that any functional genes exist in this region.

Conversely, at the junction site of chr.7, only the D2 allele was detected as a marker on the distal side of the Tg-genome junction, while the other side of the junction was intact, as expected. All the markers from mCV24854750 to mCV22532403 had been deleted on the B6 (mutant) allele. The mCV22532403 marker is about 1.2 Mb away from the Tg-genome junction. The B6 allele was present at the marker closest to the telomere, mCV22989836. These data indicate that a region greater than 1 Mb between the Tg-genome junction and mCV22532403 was deleted in the mutant chromosome. No genes have been mapped between mCV22532403 and mCV22989836 in the telomeric region of chr.7. The *Dspd* mutation loci are summarized in Figure 4C. Chr.7 was joined to the distal fragment of chr.14 by the inserted transgene, resulting in a long fusion chromosome (Fig. 4C, violet line). The proximal fragment of chr.14 was likely joined to the telomeric region of chr.7 (Fig. 4C, blue line). A region greater than 1 Mb was deleted from chr.7.

At least six genes are reported to be within the deleted region: *Cttn, Fadd, Fgf3, Fgf4, Fgf15,* and *Ccnd1.* To verify the possibility that the translocation, genomic deletion, or transgene insertion might activate genes that are not normally expressed in testicular tissue, we analyzed the expression of genes in regions flanking the mutation loci (*Dhcr7, Sftpd, Rbmxrt,* and *Ear1*) by reverse transcription-polymerase chain reaction (RT-PCR). In the *Dspd*/wt testes, these genes were expressed at nearly the same levels as in wild-type testes (data not shown).

As shown in Figure 4C, the gene that encodes the actin-binding protein cortactin, *Cttn,* was haploid deleted in *Dspd*/wt mice. The importance of cortactin in the Sertoli cell-spermatid interaction and spermiation, i.e., the release of sperm from Sertoli cells, was suggested by a previous study of rat testis [17]. Therefore, we carried out immunohistochemical analyses of cortactin in mouse seminiferous tubules. Relatively weak signals were observed at basal areas and around elongated spermatids (steps 9–15) (Fig. 5, B and C, arrows).

Importantly, dense staining was observed, especially in stage VII–VIII tubules of wild-type mice (wt/wt), which represented cortactin concentrated beside the heads of step 16 spermatids (Fig. 5A). These dense stains more likely belong to Sertoli cells than to spermatids, as referred to in a previous report [17]. Conversely, in *Dspd*/wt seminiferous tubules, localization of cortactin was disrupted. A weak diffuse signal was observed in Sertoli cells. No dense staining beside step 16 spermatids was found (Fig. 5D). There were no free dense stains (i.e., stains not associated with mature spermatids) at the seminiferous epithelium and no wandering stains in lumens.

A few sperm heads were occasionally found at the luminal edge of the seminiferous epithelium; however, they were not accompanied by the dense staining (Fig. 5D, arrows).

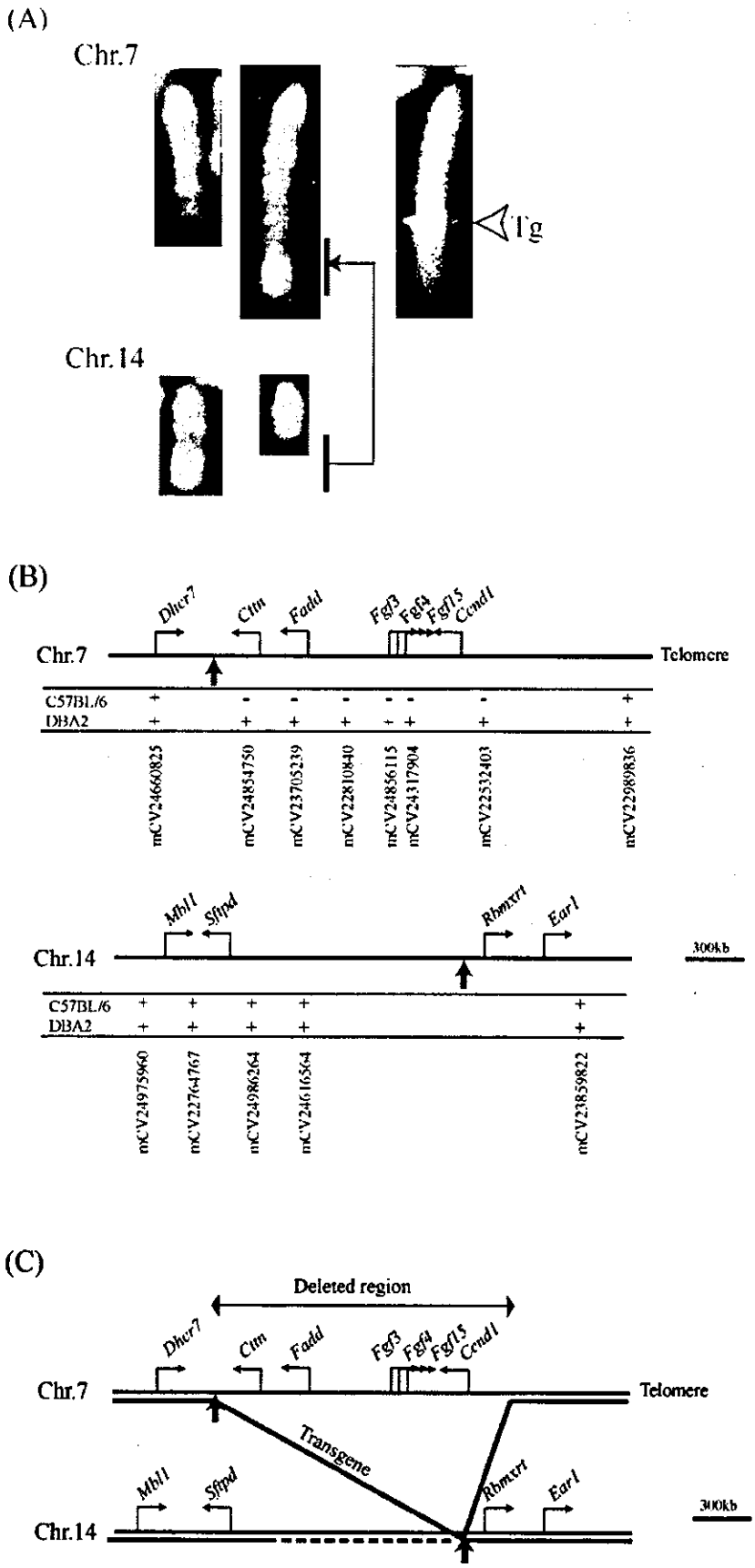

FIG. 4. Genomic analyses of *Dspd* mice. **A**) FISH analysis revealed that translocation had occurred between chr.7F and chr.14C and that the transgene had been inserted into the junction of the two chromosomes. **B**) Deletion analysis using SNP markers. Red arrows point to the transgene-genome junctions cloned from the genomic library. Genes mapped near the junctions are shown. The accession numbers of the SNPs are based on the Celera Mouse RefSNP database. + indicates the allele was present and − indicates the allele was absent. These data show a deletion of greater than 1 Mb on chr.7 of *Dspd* mice. **C**) Summary of the genomic structure of *Dspd* mutation loci. Chr.7 was joined to the distal fragment of chr.14 by the inserted transgene, resulting in a long fusion chromosome (violet line). The proximal fragment of chr.14 was likely joined to the telomeric region of chr.7 (blue line). The blue broken line represents the genomic region that could not be analyzed (see *Results*). A region greater than 1 Mb containing at least six genes (*Cttn, Fadd, Fgf3, 4, 15,* and *Ccnd1*) was found to have been deleted.

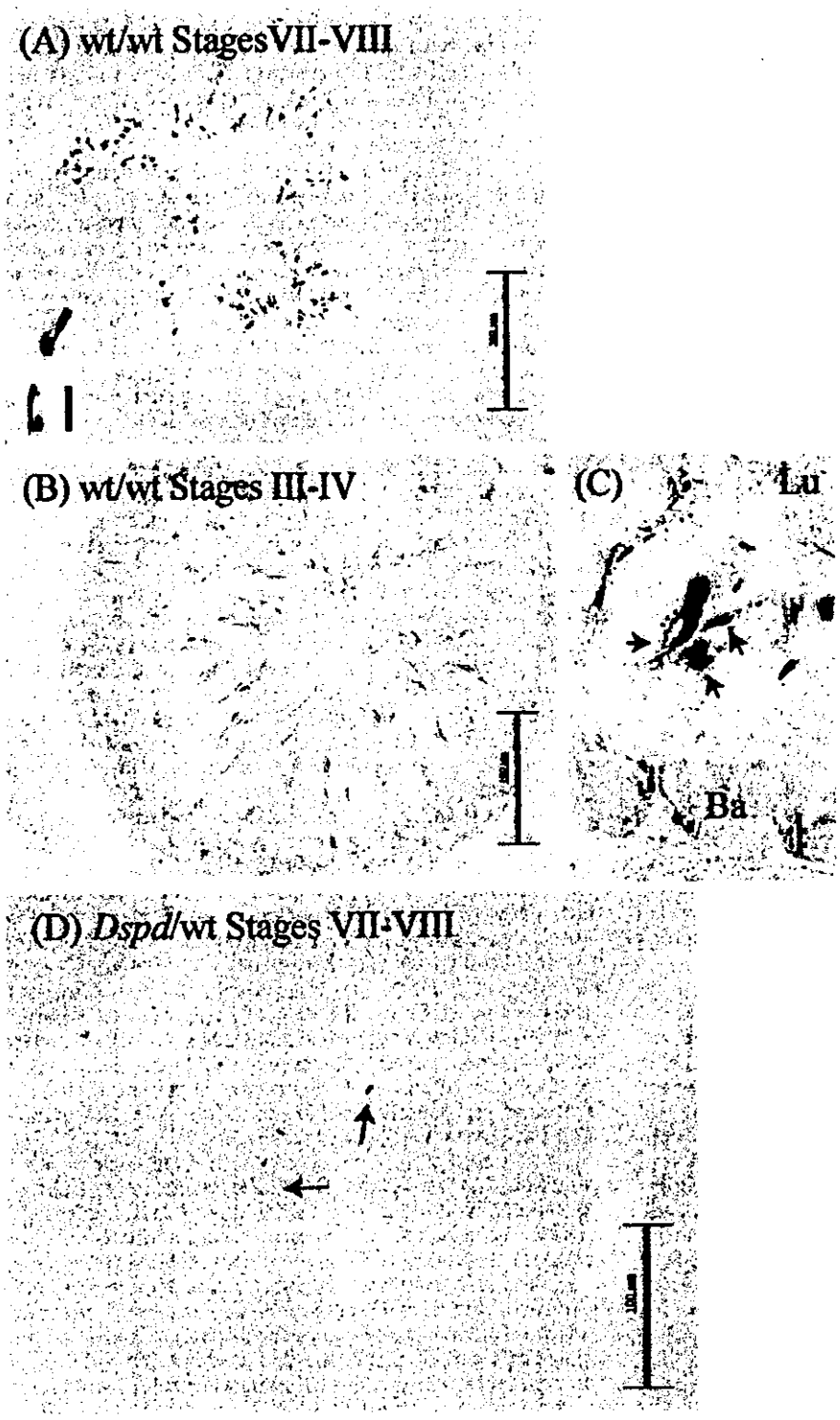

FIG. 5. Immunohistochemistry of cortactin in seminiferous tubules. (A, bar = 100 μm) Dense staining in wild-type (wt/wt) stages VII–VIII tubules demonstrates that cortactin is heavily concentrated beside step 16 spermatids. (Inset of A, bar = 5 μm) The dense stains shown at higher magnification. (B, bar = 100 μm) Weak staining was observed around the heads of elongated spermatids at early stages (stages III–IV, step 15). (C, bar = 5 μm; Lu, lumen; Ba, basal area) Cortactin localized around elongated spermatids (arrows in C). (D, bar = 100 μm) No dense staining was observed in *Dspd*/wt testis. A few condensed sperm heads were occasionally found (arrows in D) in the *Dspd*/wt seminiferous tubule (stages VII–VIII); however, they were not accompanied by dense staining.

DISCUSSION

Transgene insertions are often accompanied by genomic deletions of various sizes. It is not a simple matter to determine the size of a deletion, especially when it is coupled with a translocation and the inability to produce homozygotes due to infertility, as with *Dspd*. In this case, SNPs can be used to determine the mutant loci effectively. Using SNPs, several alleles at the translocation sites of chromosomes can be promptly checked by direct sequencing. Even if a part of the genomic assembly is imperfect, we believe that a method using SNPs is an efficient way of analyzing a mutation with a massive rearrangement of the genome.

The mutation loci of *Dspd* were mapped to chr.7F and

chr.14C. On chr.7F, a region greater than 1 Mb was deleted. By contrast, no deletions this large were found on chr.14, and no genes on chr.14 seemed to be affected by the mutation. Therefore, the deleted region of chr.7F is likely responsible for the *Dspd* phenotype. There are six well-characterized genes and at least five predicted genes (confirmed by ESTs) within the deleted region of chr.7F. The well-characterized genes are, from the proximal end, *Cttn, Fadd, Fgf3, Fgf4, Fgf15,* and *Ccnd1.* Targeted mutations of all these genes except *Cttn* have been reported [18–23]; none of the knockout mice showed any type of spermatogenic abnormality. Therefore, these five genes are unlikely the cause of the phenotype observed here, at least not independently. However, the possibility that combinations of hemizygosity might lead to unexpected effects on Sertoli or spermatogenic cells cannot be ruled out. Embryonic lethality was reported in *Fadd*-null mutant mice [18, 19], implying that homozygotes of *Dspd* (which we have not tried to make) would die in utero, if produced. The functions of the five predicted genes in this region (LOC233977, AU040576, 2210010N10Rik, BC025890, and BC019711) are unknown, making these genes possible candidates responsible for the observed phenotype.

Cttn is the most likely gene responsible for the *Dspd* phenotype because its gene product is localized where Sertoli cell-spermatid interactions occur and it has a putative function in spermiogenesis. *Cttn* encodes the 80–85-kDa actin-binding protein cortactin, which has HS1 repeats and an SH3 domain. At least three isoforms spliced with different numbers of HS1 repeats have been reported. Cortactin was initially identified as a $pp60^{Src}$ substrate [24] and a target of the Src family of protein kinases [25]. A number of cell and biochemical studies have shown that cortactin interacts with the Arp2/3 complex and N-WASP in the formation of actin filament networks [26, 27]. Therefore, cortactin connects a protein phosphorylation signal with the organization of the actin cytoskeleton. However, the functions of cortactin in vivo are not yet clear. *Dspd* is the first reported mutation affecting *Cttn* in mice.

The Sertoli cell-spermatid ES is a specialized actin-related junctional structure in Sertoli cells, which consists of actin bundles between the Sertoli plasma membrane and endoplasmic reticulum [10–12]. The functions of the ES in Sertoli cell-spermatid interactions are not clear. However, the ES is considered essential for normal morphology of elongated spermatids and for maintaining the Sertoli cell-spermatid connection until spermiation. The localization of cortactin in mouse testis resembles that of the actin-binding protein espin, a major component of the ES [28]. Cortactin is reported to interact with β_1-integrin, which is also included in the ES [17]. Furthermore, cortactin is a target of Fyn, a member of the Src family of tyrosine kinases [25, 29]. Fyn is concentrated in the ES in mouse testis, and $fyn^{-/-}$ mutant mice show an abnormality of the ES at 3–4 weeks of age [30]. These lines of evidence suggest that cortactin is included in the ES as a regulator of this actin-related junctional structure. The reduced cortactin concentration might lead to abnormalities of the ES.

Chapin et al. reported that cortactin and other junctional/cytoskeletal proteins localize around mature spermatids in rat testis and suggested that they may form some Sertoli cell-spermatid junctional structure (maybe the ES), and may function to adhere mature spermatids to Sertoli cells until spermiation [17].

The diffuse stain of cortactin in Sertoli cells and the absence of the stage-specific dense staining in the lumen and epithelium of *Dspd*/wt seminiferous tubules indicates an abnormality of the cortactin localization. We think it is likely that the haplo insufficiency of cortactin might lead to a disrupted localization of cortactin and an inefficient Sertoli cell-spermatid junctional structure and to the subsequent spermiogenesis defect.

It is interesting that *Dspd* is genetically dominant because insertional mutations generally cause a simple loss of function and do not become apparent until bred to homozygosity. However, the dosage effect of some genes encoding cytoskeletal proteins or structural components can lead to phenotypical expression. For example, the haplo insufficiency of desmoplakin, a constitutive component of desmosomal plaques, causes a striate subtype of palmoplantar keratoderma [31]. *Cttn* may be in this category.

Other possibilities might explain the genetic dominance of *Dspd.* Perhaps the deletion of part of the genome or the insertion of the transgene truncated a gene product, resulting in a dominant-negative protein that interfered with the function of its normal counterpart. To date, however, no genes or ESTs have been found at the Tg-genome junctions or at the edge of the deletion in *Dspd.* The presence of a transgene (containing a strong enhancer) might have activated genes that are not normally expressed in testicular tissue, except the intact genes neighboring the mutation loci (*Dhcr7, Sftpd, Rbmxrt,* and *Ear2*) were expressed in both wt/wt and *Dspd*/wt testes at almost the same levels (data not shown). A third possibility, genomic imprinting, can be excluded because both paternal and maternal transmission of *Dspd* appeared with the same phenotype, although the mutation locus at distal chr.7 was close to the imprinted gene cluster [32].

Follicle stimulating hormone and testosterone are major regulators of spermatogenesis. Abnormal levels of these hormones can lead to spermatogenic defects similar to *Dspd* mice [33, 34]. It is possible that secretions of these hormones might have been affected in *Dspd* mice. However, in this study, we have not examined these hormone levels. We suppose that there was little, if any, hormonal disorders in *Dspd* mutant mice for the following reasons: 1) as far as we know, the deleted genes are not involved in the regulation of these hormone levels; 2) if regulation of the hormone levels were genetically disrupted, it would be likely to affect the pubertal development of gonads; however, reproductive organs of both male and female *Dspd* mice had a normal appearance.

In this study, we isolated a mouse strain with a novel mutation that we named *Dspd.* We mapped the mutation loci to chr.7F and chr.14C and found a genomic deletion at chr.7F. We detected the absence of cortactin localization beside mature spermatids in the mutant testis and suggested that the haplo insufficiency of cortactin reduced the efficiency of the Sertoli cell-spermatid junctional structure, which resulted in the spermiogenesis defect. This is the first report of a mutation affecting cortactin in mice and the first proposal of the importance of cortactin haplo insufficiency to male infertility. Further study of *Dspd* will shed light on the molecular mechanisms of the last stage of spermatogenesis and will promote an understanding of the genetic causes of male infertility.

REFERENCES

1. Namiki M. Genetic aspects of male infertility. World J Surg 2000; 24: 1176–1179.
2. Feng HL. Molecular biology of male infertility. Arch Androl 2003; 49:19–27.

3. Cooke HJ, Saunders PT. Mouse models of male infertility. Nat Rev Genet 2002; 3:790–801.
4. Nakanishi T, Kuroiwa A, Yamada S, Isotani A, Yamashita A, Tairaka A, Hayashi T, Takagi T, Ikawa M, Matsuda Y, Okabe M. FISH analysis of 142 EGFP transgene integration sites into the mouse genome. Genomics 2002; 80:564–574.
5. Yanaka N, Kobayashi K, Wakimoto K, Yamada E, Imahie H, Imai Y, Mori C. Insertional mutation of the murine kisimo locus caused a defect in spermatogenesis. J Biol Chem 2000; 275:14791–14794.
6. MacGregor GR, Russell LD, Van Beek ME, Hanten GR, Kovac MJ, Kozak CA, Meistrich ML, Overbeek PA. Symplastic spermatids (sys): a recessive insertional mutation in mice causing a defect in spermatogenesis. Proc Natl Acad Sci U S A 1990; 87:5016–5020.
7. Pellas TC, Ramachandran B, Duncan M, Pan SS, Marone M, Chada K. Germ-cell deficient (gcd), an insertional mutation manifested as infertility in transgenic mice. Proc Natl Acad Sci U S A 1991; 88: 8787–8791.
8. Parks JE, Lee DR, Huang S, Kaproth MT. Prospects for spermatogenesis in vitro. Theriogenology 2003; 59:73–86.
9. Vogl AW, Pfeiffer DC, Mulholland D, Kimel G, Guttman J. Unique and multifunctional adhesion junctions in the testis: ectoplasmic specializations. Arch Histol Cytol 2000; 63:1–15.
10. Russell L. Observations on rat Sertoli ectoplasmic ('junctional') specializations in their association with germ cells of the rat testis. Tissue Cell 1977; 9:475–498.
11. Russell LD, Malone JP. A study of Sertoli-spermatid tubulobulbar complexes in selected mammals. Tissue Cell 1980; 12:263–285.
12. Russell LD, Goh JC, Rashed RM, Vogl AW. The consequences of actin disruption at Sertoli ectoplasmic specialization sites facing spermatids after in vivo exposure of rat testis to cytochalasin D. Biol Reprod 1988; 39:105–118.
13. Toyama Y, Hosoi I, Ichikawa S, Maruoka M, Yashiro E, Ito H, Yuasa S. Beta-estradiol 3-benzoate affects spermatogenesis in the adult mouse. Mol Cell Endocrinol 2001; 178:161–168.
14. Okutsu T, Kuroiwa Y, Kagitani F, Kai M, Aisaka K, Tsutsumi O, Kaneko Y, Yokomori K, Surani MA, Kohda T, Kaneko-Ishino T, Ishino F. Expression and imprinting status of human PEG8/IGF2AS, a paternally expressed antisense transcript from the IGF2 locus, in Wilms' tumors. J Biochem (Tokyo) 2000; 127:475–483.
15. Ogura A, Matsuda J, Asano T, Suzuki O, Yanagimachi R. Mouse oocytes injected with cryopreserved round spermatids can develop into normal offspring. J Assist Reprod Genet 1996; 13:431–434.
16. Ogura A, Ogonuki N, Inoue K, Mochida K. New microinsemination techniques for laboratory animals. Theriogenology 2003; 59:87–94.
17. Chapin RE, Wine RN, Harris MW, Borchers CH, Haseman JK. Structure and control of a cell-cell adhesion complex associated with spermiation in rat seminiferous epithelium. J Androl 2001; 22:1030–1052.
18. Yeh WC, Pompa JL, McCurrach ME, Shu HB, Elia AJ, Shahinian A, Ng M, Wakeham A, Khoo W, Mitchell K, El-Deiry WS, Lowe SW, Goeddel DV, Mak TW. FADD: essential for embryo development and signaling from some, but not all, inducers of apoptosis. Science 1998; 279:1954–1958.
19. Zhang J, Cado D, Chen A, Kabra NH, Winoto A. Fas-mediated apoptosis and activation-induced T-cell proliferation are defective in mice lacking FADD/Mort1. Nature 1998; 392:296–300.
20. Mansour SL, Goddard JM, Capecchi MR. Mice homozygous for a targeted disruption of the proto-oncogene int-2 have developmental defects in the tail and inner ear. Development 1993; 117:13–28.
21. Moon AM, Boulet AM, Capecchi MR. Normal limb development in conditional mutants of Fgf4. Development 2000; 127:989–996.
22. Ornitz DM, Itoh N. Fibroblast growth factors. Genome Biol 2001; 2: REVIEWS3005.
23. Sicinski P, Donaher JL, Parker SB, Li T, Fazeli A, Gardner H, Haslam SZ, Bronson RT, Elledge SJ, Weinberg RA. Cyclin D1 provides a link between development and oncogenesis in the retina and breast. Cell 1995; 82:621–630.
24. Wu H, Parsons JT. Cortactin, an 80/85-kilodalton pp60src substrate, is a filamentous actin-binding protein enriched in the cell cortex. J Cell Biol 1993; 120:1417–1426.
25. Thomas SM, Soriano P, Imamoto A. Specific and redundant roles of Src and Fyn in organizing the cytoskeleton. Nature 1995; 376:267–271.
26. Schafer DA. Coupling actin dynamics and membrane dynamics during endocytosis. Curr Opin Cell Biol 2002; 14:76–81.
27. Weed SA, Parsons JT. Cortactin: coupling membrane dynamics to cortical actin assembly. Oncogene 2001; 20:6418–6434.
28. Bartles JR, Wierda A, Zheng L. Identification and characterization of espin, an actin-binding protein localized to the F-actin-rich junctional plaques of Sertoli cell ectoplasmic specializations. J Cell Sci 1996; 109(pt 6):1229–1239.
29. Huang J, Asawa T, Takato T, Sakai R. Cooperative roles of Fyn and cortactin in cell migration of metastatic murine melanoma. J Biol Chem 2003; 278:48367–48376.
30. Maekawa M, Toyama Y, Yasuda M, Yagi T, Yuasa S. Fyn tyrosine kinase in Sertoli cells is involved in mouse spermatogenesis. Biol Reprod 2002; 66:211–221.
31. Armstrong DK, McKenna KE, Purkis PE, Green KJ, Eady RA, Leigh IM, Hughes AE. Haploinsufficiency of desmoplakin causes a striate subtype of palmoplantar keratoderma. Hum Mol Genet 1999; 8:143–148.
32. Beechey CV, Ball ST, Townsend KM, Jones J. The mouse chromosome 7 distal imprinting domain maps to G-bands F4/F5. Mamm Genome 1997; 8:236–240.
33. de Kretser DM, Loveland KL, Meinhardt A, Simorangkir D, Wreford N. Spermatogenesis. Hum Reprod 1998; 13(suppl 1):1–8.
34. O'Donnell L, Stanton PG, Bartles JR, Robertson DM. Sertoli cell ectoplasmic specializations in the seminiferous epithelium of the testosterone-suppressed adult rat. Biol Reprod 2000; 63:99–108.

Journal of Reproduction and Development, Vol. 50, No. 1, 2004

—Original—

Microinsemination with First-Wave Round Spermatids from Immature Male Mice

Hiromi MIKI[1,2], Jiyoung LEE[3,4], Kimiko INOUE[1,4], Narumi OGONUKI[1], Yoko NOGUCHI[5], Keiji MOCHIDA[1], Takashi KOHDA[4,6], Hiroshi NAGASHIMA[2], Fumitoshi ISHINO[3,4] and Atsuo OGURA[1,4]

[1]Institute of Physical and Chemical Research (RIKEN), 3–1–1, Koyadai, Tsukuba, Ibaraki 305–0074, [2]Meiji University Graduate School, Kanagawa 214–8571, [3]Medical Research Institute, Tokyo Medical and Dental University, 2–3–10 Kandasurugadai, Chiyoda-ku, Tokyo 101–0062, [4]CREST, JST, Saitama 332–0012, [5]National Institute of Infectious Diseases, Tokyo 162–8640, [6]Center for Biological Resources and Informatics, Tokyo Institute of Technology, Kanagawa 226–8501, Japan

Abstract. In several mammalian species, including mice, round spermatids have been used to produce normal offspring by means of microinsemination techniques. In this study, we examined whether mouse round spermatids retrieved from immature testes undergoing the first wave of spermatogenesis had acquired fertilizing ability comparable to cells from mature adults. Microinsemination with round spermatids was performed by direct injection into preactivated oocytes, as previously reported. About 60–85% of the successfully injected oocytes developed to the morula/blastocyst stage after 72 h in culture, irrespective of the age of the males (17–25 days old). After embryo transfer, normal pups were obtained from all age groups, including the day-17 group, the stage at which the first round spermatids appeared. A high correlation ($r=0.90$) was found between the birth rate and male age ($P<0.01$, Spearman rank correlation), indicating that the efficiency of producing offspring was dependent on the age of the donor males. Imprinted genes (*H19*, *Igf2*, *Meg3*, and *Igf2r*) were expressed from the correct parental alleles (maternal, paternal, maternal, and maternal, respectively) in all (n=12) day-9.5 fetuses derived from day-20 spermatids. These results clearly indicate that at least some first-wave spermatogenic cells have a normal haploid genome with the correct paternal imprint and are capable of supporting full-term embryo development, as do mature spermatozoa from adults. The use of male germ cells from immature animals may save time in the production of inbred/congenic strains and rescue male-factor infertility of early onset.

Key words: Microinsemination, Spermatogenesis, Spermatid, Genomic imprinting, Mouse

(J. Reprod. Dev. 50: 131–137, 2004)

Microinsemination, also called intracytoplasmic sperm injection (ICSI), is a technique that is used to deliver spermatozoa directly into oocytes with micromanipulation devices. This technique has provided invaluable information on several biological and molecular aspects of mammalian fertilization that could never be achieved by conventional *in vitro* fertilization (IVF). With ICSI, it was first demonstrated that sperm-egg membrane fusion can be bypassed for normal fertilization and subsequent embryo development [1–3]. With recent technical advances, immature sperm cells (spermatogenic cells) at certain stages in the testes have also been used to construct

Accepted for publiication: November 18, 2003
Correspondence: A. Ogura (e-mail: ogura@rtc.riken.go.jp)

diploid zygotes (for review, see [4, 5]). Normal offspring have been obtained by using spermatids, the haploid male germ cells produced before the completion of spermiogenesis, in mice [6], rabbits [7], rats [8], mastomys [9], rhesus monkeys [10], and humans [11]. This indicates that the spermatid genome is genetically and epigenetically competent to support full-term development, just like mature spermatozoa.

The microinsemination experiments undertaken to date have used spermatozoa or spermatogenic cells collected from mature testes. In mammals, spermatogenesis starts shortly before puberty, and the first-wave spermatogenic cells undergo meiosis and subsequent spermiogenesis in an environment that is endocrinologically and structurally different from that of the mature testis. Many of them die at the spermatocyte stage because of a phase of increased apoptosis, which is thought necessary for maturation of the seminiferous epithelium [12]. The first-wave spermatogenic cells never participate in fertilization during the normal course of sex maturation, and IVF with these cells is usually very inefficient [13]. Therefore, there is the question of whether male gametes from first-wave spermatogenesis are biologically equivalent to those from adults. In this study, we used the microinsemination technique to examine whether mouse round spermatids retrieved from immature testes have already acquired fertilizing ability comparable to cells from mature testes.

Materials and Methods

Collection of oocytes

Mature oocytes were collected from the oviducts of B6D2F1 females (SLC Co., Shizuoka, Japan) that were induced to superovulate with 7.5 IU equine chorionic gonadotropin (eCG) followed 48 h later with 7.5 IU human chronic gonadotropin (hCG). They were placed in KSOM medium [14] and treated with 0.1% bovine testicular hyaluronidase until the cumulus cells dispersed. The oocytes were placed in drops of KSOM, covered with mineral oil (Nacalai, Tokyo, Japan), and kept in plastic dishes (Falcon No. 1008, Becton Dickinson, NJ, USA) under 5% CO_2 in air, at 37 C until use.

Collection of spermatogenic cells

Spermatogenic cells were mechanically isolated from the seminiferous tubules of ICR (Clea Japan, Tokyo, Japan) or JF1 (*M. m. molossinus*) males at 16–25 days of age, as described previously [15]. The cell suspension was washed by centrifugation twice and stored in Dulbecco's phosphate-buffered saline containing 5.6 mM glucose, 5.4 mM sodium lactate, and 0.5% bovine serum albumin (BSA, fraction V, Calbiochem, CA, USA) [15] at 4 C for up to 4 h.

Microinsemination with round spermatids

Identification and injection of round spermatids were performed as previously reported [16]. About 60 min before spermatid injection, oocytes were activated by treatment with Ca^{2+}-free KSOM containing 5 mM $SrCl_2$ for 20 min. The spermatid nucleus, together with a small volume of the cytoplasm, was injected into oocytes advancing to telophase II by using a Piezo-driven micromanipulator. All the procedures were performed at room temperature (24–26 C). The injected oocytes were then kept at room temperature for about 10 minutes before they were incubated at 37 C. Oocytes that survived injection were cultured at 37 C under 5% CO_2 in air.

Embryo transfer

Embryos that reached the morula/blastocyst stage by 72 h in culture were transferred into pseudopregnant ICR females (8 to 12 weeks old) on day 2.5. Some four- to eight-cell-stage embryos were transferred into the oviducts of day-1 recipient females after 48 h in culture. On day 19.5, the recipient females were examined for the presence of fetuses, and live pups were nursed by lactating ICR females. Some females were sacrificed at day 9.5 to collect fetuses and placentas for gene expression analysis.

Allele expression analysis of imprinted genes

To see the paternal imprinting status of spermatids used for microinsemination, we performed an allele expression analysis of imprinted genes in fetuses and placentas generated by an intersubspecies cross, *i.e.*, B6D2F1 oocytes × JF1 spermatids. Polymorphisms of three imprinted genes (*H19*, *Igf2*, and *Meg3*) and one imprinted gene (*Igf2r*) between B6D2F1 and JF1 were detected by restriction fragment length polymorphism (RFLP) and length polymorphism (LP), respectively. Total RNA extraction from fetal and placental tissues, cDNA synthesis, and RT-PCR with appropriate

primer sets were performed as described previously [17].

Results

In vitro development of spermatid-injected oocytes

Round spermatids were identified in the spermatogenic cell suspension retrieved from testes at day 17 and older, but not at day 16. Conventional histological examination confirmed this finding (Fig. 1). Therefore, we performed microinsemination experiments with round spermatids from day 17–25 males, together with round spermatids from adults as controls. Most (> 90%) oocytes treated with Sr^{2+} reached telophase II with a half-protruding second polar body within 60 min. After they had been injected with round spermatids, about 80–90% of the oocytes survived and subsequently formed female and male pronuclei. The rates of cleavage and development to the morula/blastocyst stage were consistent throughout the experiments, ranging from 78 to 98% and 60 to 85%, respectively (Table 1).

In vivo development of spermatid-injected oocytes

After transfer into the oviducts or uteri of recipient females, about 20–35% of the embryos underwent implantation, irrespective of the age of the males used (Table 1). At term, normal pups were obtained from each age group, including day-17 males (Table 1, Fig. 2), the stage at which the first round spermatids appeared. Two pups (females) derived from day-17 ICR spermatids grew into normal adults and were proven fertile by natural mating. The rate of development to term per embryo transfer was very low with younger males. Then we arcsin transformed the birth rates and examined whether there was any correlation with male age. A high correlation ($r=0.90$) was found between the birth rate and male age ($P<0.01$, Spearman rank correlation) (Fig. 3), indicating that the efficiency of producing offspring from first-wave round spermatids was dependent on the age of the donor males.

Allele expression analysis of imprinted genes

To analyze imprinted gene expression, we performed round spermatid injection with JF1 males at 17, 19, 20, and 21 days of age. Term offspring were obtained from day-20 spermatids, but not from day-17, -19, or -21 spermatids. We examined the active alleles of three imprinted genes (*H19*, *Igf2*, and *Meg3*) in the term placenta derived from day-20 spermatids. All (n=4) the placentas expressed the correct allele of these three imprinted genes (maternal, paternal and maternal, respectively) (data not shown). Since it was possible that only fetuses with normal imprinted gene expression reached term, we extended our analysis to fetuses at day 9.5, the stage to which some fetuses may survive even with aberrant genomic imprinting, as seen in the development of parthenogenetic or androgenetic fetuses [18]. We

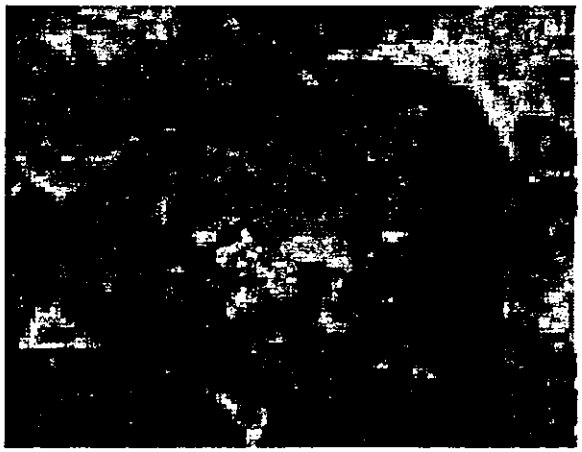

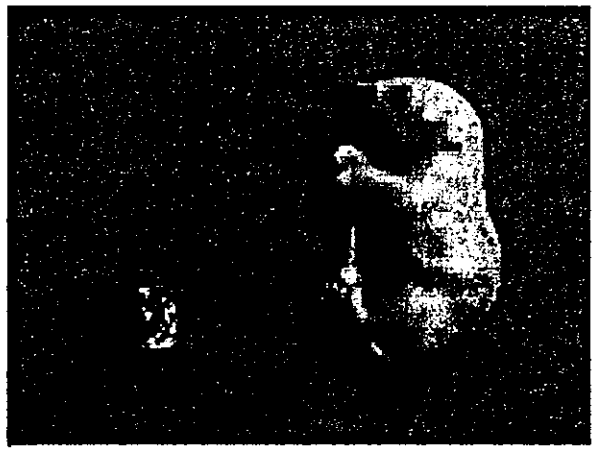

Fig. 1. The seminiferous tubules of a testis at 17 days of age. A few round spermatids that have just completed meiosis are found in some seminiferous tubules (arrows).

Fig. 2. A female pup born following microinsemination with a round spermatid at 17 days of age. It grew into a normal fertile adult.

Table 1. Embryo development *in vitro* and *in vivo* after injection with round spermatid at different ages

Age of males (days)*	No. of experiment	No. cleaved/ cultured (%)	No. (M+B**)/cultured (%)	No. transferred***	No. (%) implanted	No. (%) of fetuses
Adult	3	133 / 143 (93.0)	108 / 143 (75.5)	108	34 (31.5)	20 (18.5)
25	2	109 / 130 (83.8)	82 / 130 (63.1)	82	10 (12.2)	12 (14.6)
24	2	155 / 159 (97.5)	136 / 159 (85.5)	136	20 (14.7)	18 (13.2)
23	2	121 / 128 (94.5)	55 / 67 (82.1)	107	37 (34.6)	16 (15.0)
22	2	131 / 151 (86.8)	125 / 151 (82.8)	125	18 (14.4)	10 (8.0)
21	4	247 / 298 (82.9)	126 / 210 (60.0)	201	44 (22.0)	16 (8.0)
20	2	174 / 190 (91.6)	127 / 190 (66.8)	127	26 (20.4)	13 (10.2)
19	4	220 / 239 (92.1)	83 / 117 (70.9)	190	29 (16.3)	15 (7.9)
18	2	63 / 81 (77.8)	48 / 81 (59.3)	48	10 (25.0)	2 (4.2)
17	4	316 / 359 (88.0)	159 / 267 (59.6)	214	24 (19.4)	2 (0.9)

*Inclusive results from JF1 males at day 17, 19, 20, and 21. Results from ICR males and JF1 males were combined because the timing of the first wave spermatogenesis was the same for these strains.
**Morulae and blastocysts.
***Some of the embryos were transferred at the 4- to 8-cell stages after 48 hr in culture.

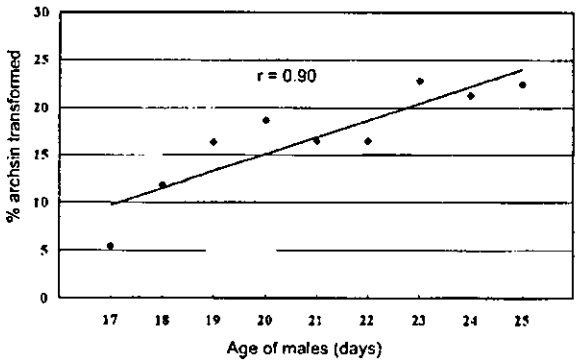

Fig. 3. The birth rates after the transfer of embryos derived from microinsemination with first-wave spermatids of different ages. The values after arcsin transformation are shown. There is a high correlation between the birth rate and the age of the donor males (r = 0.90, Spearman rank correlation).

examined twelve fetuses, including those with developmental retardation, and found that four imprinted genes (*H19*, *Igf2*, *Meg3* and *Igf2r*) were correctly expressed from each parental allele in all of the fetuses examined (Table 2, Fig. 4).

Discussion

This study examined whether the ability of first-wave spermatogenic cells to fertilize oocytes and to support embryo development is comparable to that of cells from mature testes. After injection with first-wave round spermatids, some oocytes were successfully fertilized and subsequently developed into normal term offspring. Even with day-17 spermatids, the first haploid gametes to appear in newborn male mice, we obtained two normal pups that grew into fertile adults. These findings clearly indicate that at least some first-wave spermatogenic cells have a fully functional genome, despite the difference in the testicular environments of prepubertal and adult animals. But efficiency, as measured by embryos that developed to term, was low when the youngest spermatids were used. It is important to determine whether this has a biological or technical cause.

If the younger round spermatids have a normal chromosomal constitution, as do older round spermatids, their poor developmental competency might be due to epigenetic factors. Fetal development is significantly affected by parent-specific epigenetic memory (genomic imprinting) [19]. This parent-specific memory is marked for certain genes (imprinted genes) during gametogenesis. A previous microinsemination study revealed that round spermatids from adult testes had a genomic imprinting status similar to that of mature spermatozoa [20]. The exact stage at which paternal imprinting is completed is unknown, but analysis of the DNA methylation pattern of differentially methylated regions (DMRs) of a paternally imprinted (methylated) gene, *H19*, suggested that paternal genomic imprinting occurs in primordial germ cells from day 15.5 or 16.5 of pregnancy [21, 22]. Therefore, it

Table 2. Allelic analysis of 9.5 dpc fetuses obtaind from 20 day-old JF1 males

	Fetus 1	2	3	4	5	6	7	8	9*	10*	11	12
H19	M	M	M	M**	M	M	M	M	M	M	M	M
Igf2	P	P	P	P	P	P	P	P	P	P	P	P
Meg3	M	M	M	M	M	M	M	M	M	M	M	M
Igf2r	M	M	M	M	M	M	M	M	M	M	M	M

M: maternal expression, P: paternal expression.
*Smaller than normal (about 50% of normal weight).
**With a small level (about 10%) of expression from the paternal allele.

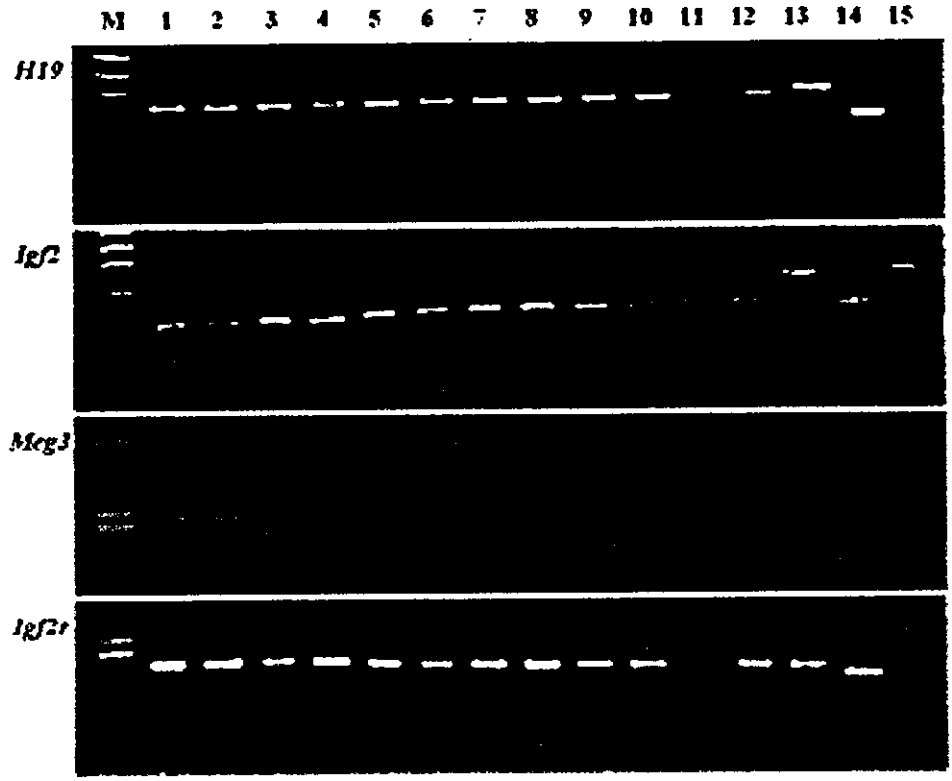

Fig. 4. Expression analysis of the *H19*, *Igf2*, *Meg3* and *Igf2r* genes in day-9.5 fetuses derived from injection with day-20 JF1 spermatids. These genes are correctly expressed from the maternal (BDF1), paternal (JF1), maternal, and maternal allele, respectively. M: marker, Lanes 1–12: BDF1 × JF1 day-9.5 fetuses from spermatid injection (cDNA), Lane 13: B6D2F1 genomic DNA, Line 14: JF1 genomic DNA, Lane 15: control JF1 × B6 day 9.5-fetus (cDNA).

is very probable that paternal imprinting memory has been completed in first-wave round spermatids, which appear about three weeks after the initiation of the paternal imprint. Our allele expression analysis of paternally imprinted genes (*H19*, *Igf2*, and *Meg3*) supported this assumption, because all the day-9.5 fetuses derived from day-20 spermatids expressed the correct alleles (maternal, paternal, and maternal, respectively). A maternally imprinted gene (*Igf2r*) was also expressed correctly. Therefore, it is unlikely that incomplete genomic imprinting affects the postimplantation development of embryos derived from first-wave round spermatids.

The population of round spermatids was relatively small in younger testes, as compared

with that of older testes. Therefore, when these younger males were used as donors, small cells other than round spermatids would be more likely to be identified erroneously and injected into oocytes. When we selected presumptive round spermatids from cell suspensions at day 17 and from adults, the accuracy as determined by the haploid chromosomal constitution within MII oocytes was 63% (12/19) and 89% (33/37), respectively (unpublished data). In our supplemental experiments, oocytes injected with cumulus cells instead of spermatids developed into morulae/blastocysts at a rate comparable to that of spermatid-derived embryos. After transfer, these 3n embryos induced the implantation reaction (decidualization), although the embryo proper, if any, was developmentally retarded (unpublished). This developmental pattern is similar to that found in this study, because embryos from younger males showed poor development to term, but showed normal development until implantation. Therefore, it is probable that technical factors, such as erroneous cell identification, are involved, at least to some extent, in the poor *in vivo* development of embryos derived from younger first-wave round spermatids.

Our results have a practical implication in mouse genetics. One of the general purposes of microinsemination techniques is the production of offspring from infertile males that cannot be rescued with conventional IVF [4]. Recently, the number of mouse strains has been increasing due to the production of new transgenic/knockout mouse strains. These genetically engineered mice may carry expected or unexpected disorders that lead to spermatogenesis failure. The use of male germ cells from immature males may rescue early-onset male-factor sterility due to spermatogenic arrest from idiopathic causes or secondary to a poor systemic condition. Furthermore, the fact that healthy fertile offspring can be obtained by microinsemination with spermatids from prepubertal males indicates that generation turnover can be accelerated during inbreeding or serial back crossing. In the mouse, each generation takes at least 3 months. With conventional superovulation, oocytes can be collected from prepubertal females at 25–30 days of age [23]. If these precociously ovulated oocytes can be fertilized with first-wave spermatids, the generation time can be shortened to 45–50 days (adding a 20-day gestation), about half of the normal generation time. To make such a technique more practical, we need to understand the biological and physical nature of oocytes and spermatogenic cells from different inbred strains, which will be an integral part of future microinsemination studies in the mouse.

Acknowledgments

This work was supported by grants from MEXT, MHLW, CREST, and the Human Science Foundation, Japan.

References

1. **Hosoi Y, Miyake M, Utsumi K, Iritani A.** Development of rabbit oocytes after microinjection of spermatozoa. Proceedings of the 11th International Congress on Animal Reproduction 1988; 3: abs.331.
2. **Goto K, Kinoshita A, Takuma Y, Ogawa K.** Fertilisation of bovine oocytes by the injection of immobilized, killed spermatozoa. *Vet Rec* 1990; 127: 517–520.
3. **Palermo G, Joris H, Debroey P, Van Steirteghem AC.** Pregnancies after intracytoplasmic injection of single spermatozoon into an oocyte. *Lancet* 1992; 340: 17–18.
4. **Ogura A, Ogonuki N, Takano K, Inoue K.** Microinsemination, nuclear transfer, and cytoplasmic transfer: the application of new reproductive engineering techniques to mouse genetics. *Mamm Genome* 2001; 12: 803–812.
5. **Ogura A, Ogonuki N, Inoue K.** Microinsemination and nuclear transfer with male germ cells. In: Cibelli JB, Lanza R, Campbell K, West MD (eds.), Principles of Cloning. San Diego: Academic Press; 2002: 175–186.
6. **Ogura A, Matsuda J, Yanagimachi R.** Birth of normal young following fertilization of mouse oocytes with round spermatids by electrofusion. *Proc Natl Acad Sci USA* 1994; 91: 7460–7462.
7. **Sofikitis NV, Miyagawa I, Agapitos E, Pasyianos P, Toda T, Hellstrom WJG, Kawamura H.** Reproductive capacity of the nucleus of the male gamete after completion of meiosis. *J Assist Reprod Genet* 1994; 11: 335–341.

8. **Hirabayashi M, Kato M, Aoto T, Ueda M, Hochi S.** Rescue of infertile transgenic rat lines by intracytoplasmic injection of cryopreserved round spermatids. *Mol Reprod Dev* 2002; 62: 295–299.
9. **Ogonuki N, Mochida K, Inoue K, Matsuda J, Yamamoto Y, Takano K, Ogura A.** Fertilization of oocytes and birth of normal pups following intracytoplasmic injection with spermatids in mastomys (Praomys coucha). *Biol Reprod* 2003; 68: 1821–1827.
10. **Hewitson L, Martinovich C, Simerly C, Takahashi D, Schatten G.** Rhesus offspring produced by intracytoplasmic injection of testicular sperm and elongated spermatids. *Fertil Steril* 2002; 77: 794–801.
11. **Tesarik J, Mendoza C, Testart J.** Viable embryos from injection of round spermatids into oocytes. *New Eng J Med* 1995; 333: 525.
12. **Billig H, Furuta I, Rivier C, Tapanainen J, Parvinen M, Hsueh A.** Apoptosis in testis germ cells: developmental changes in gonadotropin dependence and localization to selective tubular stages. *Endocrinology* 1995; 136: 5–12.
13. **Bleil JD.** In vitro fertilization. In: Wassarman PM, DePamphilis ML (eds.), Guide to Techniques in Mouse Development. San Diego: Academic Press; 1993: 253–263
14. **Lawitts JA, Biggers JD.** Culture of preimplantation embryos. *Methods Enzymol* 1993; 225: 153–164.
15. **Ogura A, Yanagimachi R.** Round spermatid nuclei injected into hamster oocytes form pronuclei and participate in syngamy. *Biol Reprod* 1993; 48: 219–225.
16. **Kimura Y, Yanagimachi R.** Mouse oocytes injected with testicular spermatozoa or round spermatids can develop into normal offspring. *Development* 1995; 121: 2397–2405.
17. **Lee J, Inoue K, Ono R, Ogonuki N, Kohda K, Kaneko-Ishino T, Ogura A, Ishino F.** Erasing genomic imprinting memory in mouse clone embryos produced from day 11.5 primordial germ cells. *Development* 2002; 129: 1807–1817.
18. **McGrath J, Solter D.** Completion of mouse embryogenesis requires both the maternal and paternal genomes. *Cell* 1984; 37: 179–83.
19. **Reik W, Walter J.** Genomic imprinting: Parental influence on the genome. *Nat Rev Genet* 2001; 2: 21–32.
20. **Shamanski FL, Kimura Y, Lavoir M-C, Pedersen RA, Yanagimachi R.** Status of genomic imprinting in mouse spermatids. *Hum Reprod* 1999; 14: 1050–1056.
21. **Ueda T, Abe K, Miura A, Yuzuriha M, Zubair M, Noguchi M, Niwa K, Kawase Y, Kono T, Matsuda Y, Fujimoto H, Shibata H, Hayashizaki Y, Sasaki H.** The paternal methylation imprint of the mouse H19 locus is acquired in the gonocyte stage during foetal testis development. *Genes Cells* 2000; 5: 649–659.
22. **Yamazaki Y, Mann MRW, Lee SS, Marh J, McCarrey JR, Yanagimachi R, Bartolomei MS.** Reprogramming of primordial germ cells begins before migration into the genital redge, making these cells inadequate donors for reproductive cloning. *Proc Natl Acad Sci USA* 2003; 100: 12207–12212.
23. **Nagy A, Gertsenstein M, Vintersten K, Behringer R.** Inducing superovulation. In: Manipulating the Mouse Embryo. 3rd ed, New York: Cold Springer Harbor Laboratory Press; 2003: 148–150.

nature genetics

Oligo-astheno-teratozoospermia in mice lacking Cnot7, a regulator of retinoid X receptor beta

Takahisa Nakamura[1], Ryoji Yao[2], Takehiko Ogawa[3], Toru Suzuki[1], Chizuru Ito[4], Naoki Tsunekawa[5], Kimiko Inoue[6], Rieko Ajima[1], Takashi Miyasaka[1], Yutaka Yoshida[1], Atsuo Ogura[6], Kiyotaka Toshimori[4], Toshiaki Noce[5], Tadashi Yamamoto[1] & Tetsuo Noda[2,7,8]

Spermatogenesis is a complex process that involves cooperation of germ cells and testicular somatic cells. Various genetic disorders lead to impaired spermatogenesis, defective sperm function and male infertility[1]. Here we show that *Cnot7*$^{-/-}$ males are sterile owing to oligo-astheno-teratozoospermia, suggesting that Cnot7, a CCR4-associated transcriptional cofactor[2], is essential for spermatogenesis. Maturation of spermatids is unsynchronized and impaired in seminiferous tubules of *Cnot7*$^{-/-}$ mice. Transplantation of spermatogonial stem cells from male *Cnot7*$^{-/-}$ mice to seminiferous tubules of *Kit* mutant mice (*Kit*$^{W/W\text{-}v}$) restores spermatogenesis, suggesting that the function of testicular somatic cells is damaged in the *Cnot7*$^{-/-}$ condition. The testicular phenotypes of *Cnot7*$^{-/-}$ mice are similar to those of mice deficient in retinoid X receptor beta (*Rxrb*)[3]. We further show that Cnot7 binds the AF-1 domain of Rxrb and that Rxrb malfunctions in the absence of Cnot7. Therefore, Cnot7 seems to function as a coregulator of Rxrb in testicular somatic cells and is thus involved in spermatogenesis.

Genetic analyses in yeast suggest that CAF1, a component of the CCR4-NOT complex, has multiple roles in regulating transcription[4]. In addition, proteins in the CCR4-NOT complex are involved in mRNA metabolism in yeast[5,6]. Two mammalian homologs of yeast CAF1 are known: Cnot7 (also called CAF1) and Cnot8 (also called CALIF)[7,8]. Both are expressed in a variety of tissues, with relatively high expression of Cnot7 in lung, liver and thyroid gland[7,8]. Cnot7 interacts with members of the TOB-BTG antiproliferative family, which comprises Tob1, Tob2, Btg1, Btg2 (also called PC3 and TIS21), Btg3 (also called ANA) and Btg4 (also called PC3B; refs. 7,9,10). The proteins of this family are implicated in regulation of transcription[11–14].

To elucidate the physiological role of mammalian Cnot7, we produced mutant mice lacking the gene *Cnot7* by means of homologous recombination (**Fig. 1a–d**). Homozygous *Cnot7* knockout (*Cnot7*$^{-/-}$) mice were alive at birth and born at the predicted mendelian frequency. Adult *Cnot7*$^{-/-}$ mice had normal health, size and behavior, except that male *Cnot7*$^{-/-}$ mice were sterile. *Cnot7*$^{+/-}$ males had normal fertility and *Cnot7*$^{-/-}$ females produced average-size litters (6.3 ± 2.1 offspring per litter; $n = 14$ litters).

There were no gross anatomical differences in the seminal vesicles and prostates among *Cnot7*$^{+/+}$, *Cnot7*$^{+/-}$ and *Cnot7*$^{-/-}$ males, but the testes of *Cnot7*$^{-/-}$ mice were smaller than those of *Cnot7*$^{+/+}$ or *Cnot7*$^{+/-}$ mice (**Fig. 1e**). *Cnot7*$^{-/-}$ mice produced only 7% as much sperm as *Cnot7*$^{+/+}$ or *Cnot7*$^{+/-}$ mice (**Fig. 1f**), and their spermatozoa beat less vigorously and generated less forward momentum (**Fig. 1g**). Almost all spermatozoa from *Cnot7*$^{-/-}$ mice had irregularly shaped heads, abnormally arranged mitochondria and erroneously attached flagella (**Fig. 1h,i**). Electron microscopic analysis detected ultrastructural components, such as condensed chromatin, acrosomes and flagella, including axoneme, mitochondrial sheath, outer dense fibers and fibrous sheath, in spermatozoa from *Cnot7*$^{-/-}$ mice. But their arrangements were irregular and maturation of sperm was abnormal (**Fig. 1i**). The degree of morphological irregularity varied: spermatozoa of *Cnot7*$^{-/-}$ mice were round-headed (73%), tapered-headed (20%), symplast (5%) or nearly normal (2%). We also observed malformation of spermatids in the seminiferous tubules (see **Fig. 3d**). Taken together, these data indicate that oligo-astheno-teratozoospermia (low sperm number and motility and abnormal sperm morphology) underlies the sterility of *Cnot7*$^{-/-}$ males.

To further analyze sperm competence for fertilization, we carried out *in vitro* fertilization (IVF) and intracytoplasmic sperm injection (ICSI) experiments. For the IVF experiment, we freed oocytes from cumulus cells and the zona pellucida, because epididymal spermatozoa of *Cnot7*$^{-/-}$ mice had poor motility and were unable to penetrate these egg layers. Even under these experimental conditions, spermatozoa of *Cnot7*$^{-/-}$ mice hardly fertilized oocytes, whereas *Cnot7*$^{+/-}$ spermatozoa had normal fertilizing ability (**Table 1**). Direct injection of

[1]Division of Oncology, Institute of Medical Science, University of Tokyo, Tokyo 108-8639, Japan. [2]Department of Cell Biology, Japanese Foundation for Cancer Research (JFCR) Cancer Institute, Tokyo 170-8455, Japan. [3]Department of Urology, School of Medicine, Yokohama City University, Kanagawa 236-0004, Japan. [4]Department of Anatomy and Developmental Biology, Graduate School of Medicine, Chiba University, Chiba 260-8670, Japan. [5]Mitsubishi Kagaku Institute of Life Sciences, Tokyo 194-8511, Japan. [6]RIKEN Bioresource Center, Ibaraki 305-0074, Japan. [7]Center for Translational and Advanced Animal Research on Human Disease, Tohoku University School of Medicine, Miyagi 980-8575, Japan. [8]Mouse Functional Genomics Research Group, RIKEN Genomic Sciences Center, Kanagawa 244-0804, Japan. Correspondence should be addressed to T.Y. (tyamamot@ims.u-tokyo.ac.jp) or T. Noda (tnoda@ims.u-tokyo.ac.jp).

Published online 25 April 2004; doi:10.1038/ng1344